Kinetic studies of keto-enol and other tautomeric equilibria by flash photolysis

Jakob Wirz
Department of Chemistry
University of Basel
Klingelbergstrasse 80, CH-4056 Basel, Switzerland

1 Introduction

Erlenmeyer was first to consider enols as hypothetical primary intermediates in a paper published in 1880 on the dehydration of glycols.[1] Ketones are inert towards electrophilic reagents, in contrast to their highly reactive enol tautomers. However, the equilibrium concentrations of simple enols are generally quite low. That of 2-propenol, for example, amounts to only a few ppb in aqueous solutions

of acetone. Nevertheless, many important reactions of ketones proceed via the more reactive enols, and enolization is then generally rate-determining. Such a mechanism was put forth in 1905 by Lapworth,[2] who showed that the bromination rate of acetone in aqueous acid was independent of bromine concentration and concluded that the reaction is initiated by acid-catalyzed enolization, followed by fast trapping of the enol by bromine (Scheme 1). This was the first time that a mechanistic hypothesis was put forth on the basis of an observed rate law. More recent work has shown that the reaction of bromine with various acetophenone enols in aqueous solution takes place at nearly, but not quite, diffusion-controlled rates.[3]

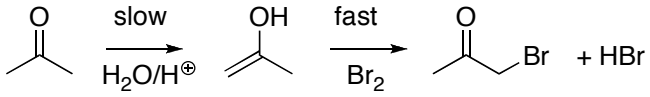

Scheme 1

In 1978, we observed that flash photolysis of butyrophenone produced acetophenone enol as a transient intermediate, which allowed us to determine the acidity constant K_a^E of the enol from the pH–rate profile (section 2.4) of its decay in aqueous base.[4] That work was a sideline of studies aimed at the characterization of biradical intermediates in Norrish Type II reactions and we had no intentions to pursue it any further. Enter Jerry Kresge, who had previously determined the ketonization kinetics of several enols using fast thermal methods for their generation. He immediately realized the potential of the photochemical approach to study keto–enol equilibria and quickly convinced us that this technique should be further exploited. We were more than happy to follow suit and to cooperate with this distinguished, inspiring and enthusing chemist and his cherished wife Yvonne Chiang, who sadly passed away last year. Over the years, this collaboration developed into an intimate friendship of our families. The present chapter is an account of what has been achieved. Several reviews in this area appeared in the years up to 1998.[5-10]

The enol tautomers of many ketones and aldehydes, carboxylic acids, esters and amides, ketenes, as well as the keto tautomers of phenols have since all been generated by flash photolysis to determine the pH–rate profiles for keto-enol interconversion. Equilibrium constants of enolization, K_E, were determined accurately as the ratio of the rate constants of enolization, k^E, and of ketonization, k^K, Equation 1.

$$K_E = k^E/k^K$$

Equation 1. Kinetic determination of equilibrium constants of enolization

Strong bases in dry solvents are usually used in organic synthesis to generate reactive enol anions from ketones. Nevertheless, the kinetic studies discussed here were mostly performed on aqueous solutions. Apart from the relevance of this medium for biochemical reactions and green chemistry, it has the advantage

of a well-defined pH-scale permitting quantitative studies of acid and base catalysis.

2 Methods

2.1 Flash Photolysis

The technique of flash photolysis, introduced in 1949 by Norrish and Porter,[11] now covers time scales ranging from a few femtoseconds to seconds and has become a ubiquitous tool to study reactive intermediates. Most commonly, light induced changes in UV-Vis optical absorption are monitored, either at a single wavelength (kinetic mode) or spectrographically at a given delay with respect to the light pulse used for excitation (spectrographic mode, pump–probe spectroscopy). Instruments of a conventional design,[12] which employ an electric discharge to produce a strong light flash of sub-millisecond duration, usually have sufficient time resolution and are then most suitable to study the kinetics of keto–enol tautomerization reactions. Nowadays, instruments using a Q-switched laser as an excitation source having durations of a few nanoseconds (laser flash photolysis) are much more widespread. These techniques are well-known, and their properties, pitfalls and limitations have been described.[13-15]

2.2 Derivation of the Rate Law for Keto–Enol Equilibration

Activation energies for unimolecular 1,3-hydrogen shifts connecting ketones and enols are prohibitive, so that thermodynamically unstable enols can survive indefinitely in the gas phase or in dry, aprotic solvents. Ketones are weak carbon acids and oxygen bases, enols are oxygen acids and carbon bases. In aqueous solution, keto–enol tautomerization proceeds by proton transfer involving solvent water. In the absence of buffers, three reaction pathways compete, as shown in Scheme 2.

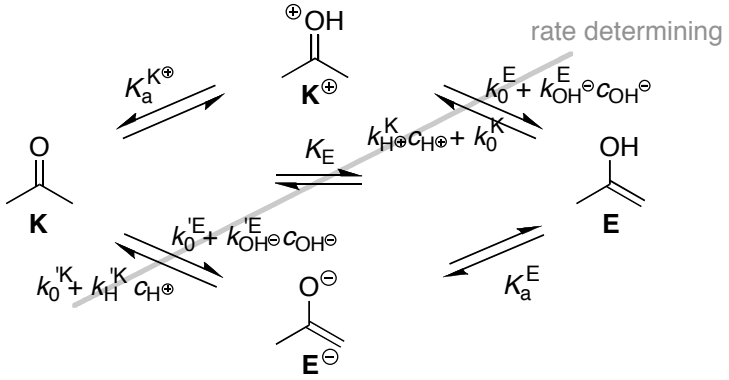

Scheme 2. Acid-, base-, and "uncatalyzed" reaction paths of keto–enol tautomerism.

Four species participate in the tautomerization reaction, the ketone (**K**, e.g., acetone), the protonated ketone ($\mathbf{K}^{\oplus}$), the enol (**E**), and its anion ($\mathbf{E}^{\ominus}$). These species are connected through two thermodynamic cycles. The Gibbs free

energies for the individual elementary reactions r of any cycle must add up to naught, Equation 2.

$$\Sigma\Delta_r G^\circ = 2.3RT\Sigma \mathrm{p}K_r = 0$$

Equation 2

For the cycle $\mathbf{K} \rightarrow \mathbf{E} \rightarrow \mathbf{E}^{\ominus} + \mathrm{H}^{\oplus} \rightarrow \mathbf{K}$ we get $\mathrm{p}K_\mathrm{E} + \mathrm{p}K_\mathrm{a}^\mathrm{E} - \mathrm{p}K_\mathrm{a}^\mathrm{K} = 0$, where K_E is the equilibrium constant of enolization and K_a^E and K_a^K are the acidity constants of **E** and **K**, respectively; K_a^K is defined in the direction opposite to the last process of the cycle so that $\mathrm{p}K_\mathrm{a}^\mathrm{K}$ must be subtracted. Similarly, the equilibrium constant for carbon deprotonation of the protonated ketone, $\mathbf{K}^{\oplus} \rightarrow \mathbf{E} + \mathrm{H}^{\oplus}$, can be replaced by $\mathrm{p}K_\mathrm{E} + \mathrm{p}K_\mathrm{a}^{\mathrm{K}\oplus}$, where $\mathrm{p}K_\mathrm{a}^{\mathrm{K}\oplus}$is the acidity constant of $\mathbf{K}^{\oplus}$. Thus, the equilibrium properties of Scheme 2 are fully defined by the three equilibrium constants K_E, K_a^E, and $K_\mathrm{a}^{\mathrm{K}\oplus}$.

We turn to the kinetic parameters. When an enol **E** is rapidly generated in a concentration $c_\mathrm{E}(t = 0)$ exceeding its equilibrium concentration $c_\mathrm{E}(\infty)$, the decrease of $c_\mathrm{E}(t)$ may be followed in time by, for example, some absorbance change as in flash photolysis. Deprotonation or protonation of carbon atoms is generally slow relative to the equilibration of oxygen acids with their conjugate bases. Therefore, carbon acids and bases have been called pseudo-acids and pseudo-bases. Proton transfer reactions involving carbon are the rate-determining elementary steps of the tautomerization reactions. A shaded oblique line is drawn across these reactions in Scheme 2. Thus we posit that the protonation equilibria on oxygen that are associated with the ionization constants K_a^E and $K_\mathrm{a}^{\mathrm{K}\oplus}$ are established at all times during the much slower tautomerization reactions. This assumption leads to a pH-dependent first-order rate law for keto–enol tautomerization reactions, Equation 14, that will be derived below and is found to hold in general. The pre-equilibrium assumption adopted for oxygen acids is, thereby, amply justified.

We define equilibrium constants as concentration quotients, as in Equation 3 for K_a^E and $K_\mathrm{a}^{\mathrm{K}\oplus}$. Provided that the experiments are done at low and constant ionic strengths, $I \leq 0.1$ M, these can be converted to thermodynamic constants, K_a°, using known or estimated activity coefficients.[16]

$$K_\mathrm{a}^\mathrm{E} = c_\mathrm{E}{}^{\ominus}(t)\, c_{\mathrm{H}\oplus}/c_\mathrm{E}(t) \text{ and } K_\mathrm{a}^{\mathrm{K}\oplus} = c_\mathrm{K}(t)\, c_{\mathrm{H}\oplus}/c_{\mathrm{K}\oplus}(t)$$

Equation 3

The total concentration of the enol and its anion is $c_{\mathrm{E,tot}}(t) \equiv c_\mathrm{E}(t) + c_\mathrm{E}{}^{\ominus}(t)$; inserting Equation 3 we can express the concentrations c_E and $c_\mathrm{E}{}^{\ominus}$ as a function of proton concentration $c_{\mathrm{H}\oplus}$, Equation 4.

$$c_\mathrm{E}(t) = \frac{c_{\mathrm{H}^\oplus}}{K_\mathrm{a}^\mathrm{E} + c_{\mathrm{H}^\oplus}} c_{\mathrm{E,tot}}(t) \quad \text{and} \quad c_{\mathrm{E}^\ominus}(t) = \frac{K_\mathrm{a}^\mathrm{E}}{K_\mathrm{a}^\mathrm{E} + c_{\mathrm{H}^\oplus}} c_{\mathrm{E,tot}}(t)$$

Equation 4

Protons and hydroxyl ions are not consumed by the reaction $\mathbf{K} \rightleftharpoons \mathbf{E}$. A temporary shift in the relative concentrations of **K** and **E** may, however, lead to a

change in proton concentration $c_{H\oplus}$ due to rapid equilibration with $\mathbf{K}^{\oplus}$ and $\mathbf{E}^{\ominus}$, respectively. To avoid this complication, the conditions are generally chosen such that $c_{H\oplus}$ remains essentially constant during the reaction by using either a large excess of acid or base, or by the addition of buffers in near neutral solutions (pH = 7 ± 4). However, the addition of buffers usually accelerates the rates of tautomerization. We first consider reactions taking place in wholly aqueous solutions, that is, in the absence of buffers. The handling of rate constants obtained with buffered solutions will be discussed in section 2.5.

To derive the general rate law for keto–enol equilibration, we consider each of the rate-determining elementary reaction steps shown in Scheme 2 separately, beginning with enol ketonization reactions. The relevant rate constants for the rate-determining ketonization reactions are $k_{H\oplus}^{K}$ and k_0^{K} for C-protonation of **E** by $H^{\oplus}$ and solvent water, respectively, and $k_{H\oplus}'^{K}$ and $k_0'^{K}$ for C-protonation of $\mathbf{E}^{\ominus}$ by $H^{\oplus}$ and water (Scheme 2). We use primed symbols k' for the rate constants referring to ketonization of the anion $\mathbf{E}^{\ominus}$. As we shall see in a moment (Equation 7), the terms k_0^{K} and $k_{H\oplus}'^{K}K_a^{E}$ are both independent of pH and may be combined to a single term k_{uc}^{K}. The associated, seemingly "uncatalyzed" reactions are therefore kinetically indistinguishable and additional information is required to determine, which of the corresponding mechanisms is the dominant one (see section 4.2). We assume that the rate-determining reactions shown in Scheme 2 are elementary reactions, so that the corresponding rate laws are equal to the product of a rate constant and the concentrations of the reacting species.

a) *Acid-catalyzed ketonization*: The rate for ketone formation by carbon protonation of the enol **E** is given by Equation 5, where the right-hand expression is obtained by substituting $c_E(t)$ using Equation 4.

$$v_{H\oplus}^{K} = k_{H\oplus}^{K} c_{H\oplus} c_E(t) = k_{H\oplus}^{K} c_{H\oplus} \frac{c_{H\oplus}}{K_a^{E} + c_{H\oplus}} c_{E,tot}(t)$$

Equation 5

b) *Base-catalyzed ketonization*: Pre-equilibrium ionization of **E** generates the more reactive anion $\mathbf{E}^{\ominus}$, which may be protonated on carbon by the general acid water in the rate-determining step, Equation 6. For pH-values well below pK_a^{E}, the concentration $c_{H\oplus}$ is much greater than K_a^{E}, so that it may be neglected in the denominator of Equation 6. The rate of this reaction is then inversely proportional to $c_{H\oplus}$, i.e., proportional to $c_{OH^{\ominus}}$. This "apparent" base catalysis saturates at pH-values above pK_a^{E}, when **E** is converted to $\mathbf{E}^{\ominus}$. The concentration $c_{H\oplus}$ then becomes much smaller than K_a^{E} and may be neglected in the denominator of Equation 6.

$$v_{OH^{\ominus}}^{K} = k_0'^{K} c_{E^{\ominus}}(t) = k_0'^{K} \frac{K_a^{E}}{K_a^{E} + c_{H\oplus}} c_{E,tot}(t)$$

Equation 6

c) *"Uncatalyzed" ketonization*. At pH-values near neutral, a pH-independent rate of ketonization is frequently observed, which may be attributed to several different mechanisms (see section 4.2): carbon protonation of **E** by water or a concerted transfer of the enol proton to carbon through one or more solvent molecules, and carbon protonation of $\mathbf{E}^{\ominus}$ by the proton, Equation 7. For pH << pK_a^E, the right-hand expression becomes independent of $c_{H\oplus}$.

$$v_0^K = k_0^K c_E(t) + k_{H\oplus}^{'K} c_{H\oplus} c_{E^\ominus}(t) = \left(k_0^K + k_{H\oplus}^{'K} K_a^E\right) \frac{c_{H\oplus}}{K_a^E + c_{H\oplus}} c_{E,tot}(t)$$

Equation 7

Summing up the rates of these competing reaction paths, Equations 5–7, one obtains the total rate of enol ketonization, Equation 8. Note that v^K refers exclusively to the forward reaction **E** → **K**.

$$v^K = \left[\left(k_0^K + k_{H\oplus}^{'K} K_a^E\right) + k_{H\oplus}^K c_{H\oplus} + k_0^{'K} \frac{K_a^E}{c_{H\oplus}}\right] \frac{c_{H\oplus}}{K_a^E + c_{H\oplus}} c_{E,tot}(t) = k^K c_{E,tot}(t)$$

Equation 8. Rate of ketonization

The rather complex expression preceding $c_{E,tot}(t)$ is nothing but a collection of constants for a given proton concentration $c_{H\oplus}$. Thus, Equation 8 represents a first-order rate law with a pH-dependent rate constant k^K.
The three independent rate constants $k_{H\oplus}{}^K$, $k_0{}'^K$ and $k_{uc}{}^K = k_0{}^K + k_{H\oplus}{}'^K K_a{}^E$ fully determine the kinetic properties of Scheme 2, because the rate constants k_i^E for enolization are related[a] to those of the reverse reactions, Equation 9, where K_w is the ionization constant of water. We use primed symbols for the enolization of the neutral ketone **K**. In the rate equation for enolization, the terms $k_0{}'^E$ and $k_{OH^\ominus}{}^E K_w/K_a{}^{K\oplus}$ are kinetically indistinguishable (see Equation 10 below).

$$\text{a) } k_0^E = K_E K_a^{K^\oplus} k_{H\oplus}^K, \quad \text{b) } k_{OH^\ominus}^E = K_E K_a^{K^\oplus} k_0^K / K_w,$$
$$\text{c) } k_0^{'E} = K_a^K k_{H\oplus}^{'K}, \qquad \text{d) } k_{OH^\ominus}^{'E} = K_a^K k_0^{'K} / K_w$$

Equation 9. Thermodynamic relations between the rate constants of ketonization and enolization.

The rate of the reverse reactions, Equation 10, is derived in the same way using $c_{K,tot}(t) \equiv c_{K\oplus}(t) + c_K(t)$ and the ionization product of water, $K_w = 1.59 \times 10^{-14}$ M^2 ($I = 0.1$ M), to replace $c_{OH^\ominus}$ by $K_w/c_{H\oplus}$.

$$v^E = \left[\left(k_0^{'E} + k_{OH^\ominus}^E \frac{K_w}{K_a^{K^\oplus}}\right) + \frac{k_0^E}{K_a^{K^\oplus}} c_{H\oplus} + k_{OH^\ominus}^{'E} \frac{K_w}{c_{H\oplus}}\right] \frac{K_a^{K^\oplus}}{K_a^{K^\oplus} + c_{H\oplus}} c_{K,tot}(t)$$

Equation 10.

---

[a] In a system of connected reversible reactions at equilibrium, each reversible reaction is individually at equilibrium. This is the principle of microscopic reversibility or its corollary, the principle of detailed balance.

Replacement of the rate constants k_i^{E} in Equation 10 by those of the reverse reactions k_i^{K} using Equation 9 gives Equation 11. Most ketones are very weak bases, $pK_a^{K\oplus} < 0$. Hence, $c_{H\oplus}$ in the denominator of Equation 11 may be neglected relative to $K_a^{K\oplus}$ in the normal pH-range, i.e., the ratio $K_a^{K\oplus}/(K_a^{K\oplus} + c_{H\oplus})$ is unity.

$$v^{E} = \left[\left(k_0^{K} + k'^{K}_{H\oplus} K_a^{E} \right) + k^{K}_{H\oplus} c_{H\oplus} + k'^{K}_{0} \frac{K_a^{E}}{c_{H\oplus}} \right] K_E \frac{K_a^{K\oplus}}{K_a^{K\oplus} + c_{H\oplus}} c_{K,tot}(t) = k^{E} c_{K,tot}(t)$$

Equation 11. Rate of enolization

The observed rate law. Starting from an excess enol concentration at time $t = 0$, the observable decay of total enol concentration in time, Equation 12, is equal to the difference between the ketonization rate of the enol, v^{K} (Equation 8), and the enolization rate of the ketone, v^{E} (Equation 11). Equilibrium ($t = \infty$) is reached when $v^{K} = v^{E}$, i.e., when $-dc_{E,tot}(t)/dt = 0$.

$$-dc_{E,tot}(t) / dt = v^{K} - v^{E} = k^{K} c_{E,tot}(t) - k^{E} c_{K,tot}(t)$$

Equation 12

The time-dependent concentrations $c_{E,tot}(t)$ and $c_{K,tot}(t)$ are related by mass conservation, $c_{E,tot}(t) + c_{K,tot}(t) = c_{E,tot}(\infty) + c_{K,tot}(\infty) = \text{const}$. Substituting $c_{K,tot}(t)$ by $c_{E,tot}(\infty) + c_{K,tot}(\infty) - c_{E,tot}(t)$ and using the relation $c_{E,tot}(\infty)/c_{K,tot}(\infty) = k^{E}/k^{K}$ one obtains Equation 13.

$$-dc_{E,tot}(t) / dt = \left(k^{E} + k^{K} \right) \left[c_{E,tot}(t) - c_{E,tot}(\infty) \right]$$

Equation 13. Differential rate law for the decay of enol

Integration gives the rate law for the decay of enol to its equilibrium concentration $c_{E,tot}(\infty)$, Equation 14.

$$c_{E,tot}(t) = \left[c_{E,tot}(0) - c_{E,tot}(\infty) \right] e^{-\left(k^{E} + k^{K} \right) t} + c_{E,tot}(\infty)$$

Equation 14. Integrated rate law for the decay of excess enol

Thus the approach to equilibrium always follows a first-order rate law, Equation 14, with the pH-dependent rate constant $k_{obs} = k^{E} + k^{K}$. Figure 1 shows the concentration changes in time starting from a 1M solution of pure enol (full line) and of pure ketone (dashed line). The individual, unidirectional rate constants k^{E} and k^{K} can be determined as follows: For most ketones the equilibrium enol concentration is quite small, i.e., $K_E = c_E(\infty)/c_K(\infty) << 1$. Hence $k^{E} << k^{K}$ (Equation 1), so that enol ketonization is practically irreversible and k^{E} may be neglected, $k_{obs} \approx k^{K}$. The rate constant of enolization k^{E}, on the other hand, is equal to the observed rate constant of reactions for which enolization is rate-determining, such as ketone bromination (Scheme 2).

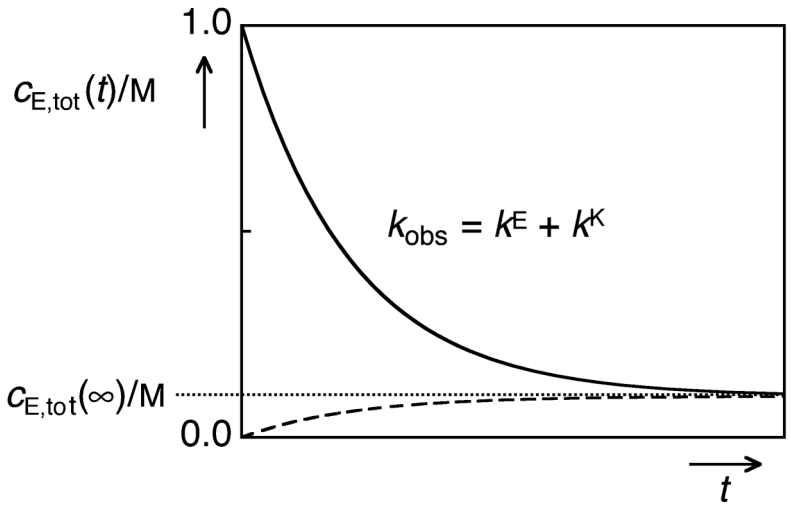

Figure 1. Time-dependent concentrations of $c_{E,tot}(t)$, starting from pure enol (full line), and pure ketone (dashed line), Equation 14.

2.3 Halogen Titration Method

Some ketones such as β-dicarbonyls contain substantial amounts of the enol at equilibrium. For example, acetylacetone in aqueous solutions contains 13% of 4-hydroxypent-3-en-2-one, which is stabilized both by an intramolecular hydrogen bond and the inductive effect of the remaining carbonyl group.[17] When bromine is added to such a solution, a portion is initially consumed very rapidly by the enol that is already present at equilibrium. The ketone remaining after consumption of the enol reacts more slowly via rate-determining enolization. The slow consumption of bromine is readily measured by optical absorption. In acidic solutions containing a large excess of the ketone the slow reaction follows a zero-order rate law; the rate is independent of bromine concentration, because any enol formed is rapidly trapped by bromine (Scheme 1). In this case, the amount of enol present at equilibrium may be determined as the difference between the amount of bromine added and that determined by extrapolation of the observed rate law to time zero, as is shown schematically in Figure 2.

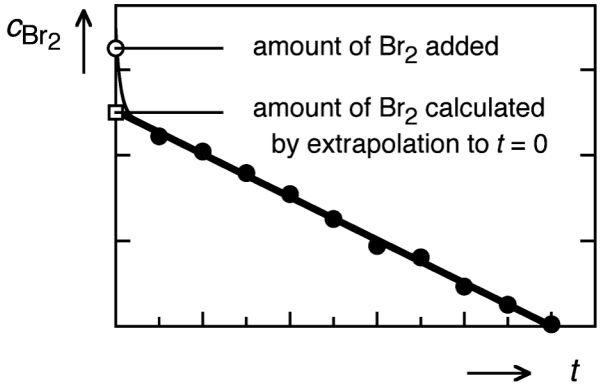

Figure 2. Bromine titration method.

This technique, called "bromine titration method", was extensively used by K. H. Meyer in the early twentieth century.[18] It was later extended to determine the enol content of simple ketones using faster flow methods combined with more sensitive potentiometric measurements of bromine uptake, but this technique sometimes produced apparent enol contents that were far too high, such as the enol content of acetone of 2.5×10^{-4} % that is frequently quoted in older textbooks of organic chemistry. The excessive values so obtained have been attributed to the presence of small amounts of impurities reacting with bromine.

2.4 pH–Rate Profiles

The dependencies of k_{obs} (Equation 14), k^E (Equation 11), and k^K (Equation 8) on proton concentration are usually displayed in log–log plots called pH–rate profiles, which allow one to identify the reaction paths dominating at various pH-values as well as the parameters of the rate law, namely the acidity constants K_a and the elementary rate constants of the rate-determining steps. Figure 3 shows pH–rate profiles of k^E (dashed line), k^K (thin full line, coincides with k_{obs} below pH 17) and $k_{obs} = k^E + k^K$ (thick grey line), which were plotted using Equation 8 and Equation 11 with the six relevant kinetic and thermodynamic parameters that have been determined for acetophenone (see Table 1 in section 3).[4, 19-23]

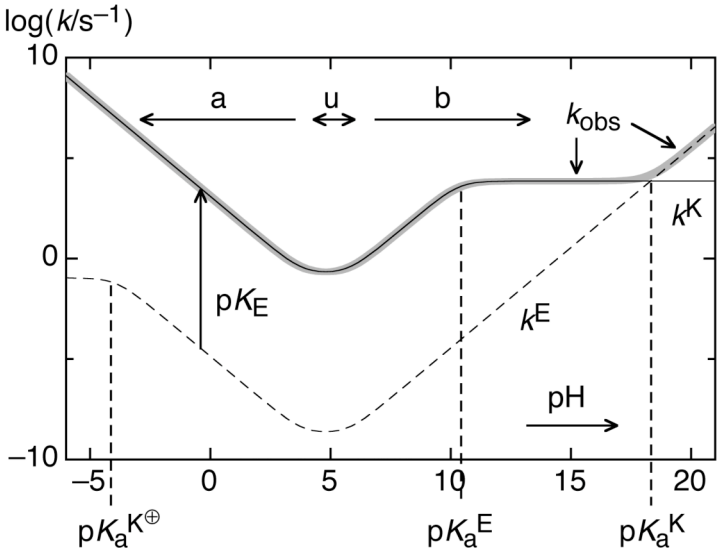

Figure 3. pH–Rate profiles for k^K (—, Equation 8), k^E (- - -, Equation 11) and $k_{obs} = k^K + k^E$ (▬) of acetophenone in aqueous solution.

It is worth spending some time to interpret and digest the curves shown in Figure 3. The acid-catalyzed reaction paths dominate at pH-values below 3 (marked by the symbol „a“). In region "a", the slope of the curves equals –1 because the rate constants k^E and k^K are directly proportional to acid concentration $c_{H\oplus}$. This is due to the dominant terms $k_{H\oplus}{}^K c_{H\oplus}$ of Equation 8 and Equation 11. Because the acidity constant of enols, $K_a{}^E$, is usually much smaller than $c_{H\oplus}$ at pH < 3, the

ratio $c_{H\oplus}/(K_a^E + c_{H\oplus})$ of Equation 8 amounts to unity. On the other hand, protonated ketones are very strong acids, $pK_a^{K\oplus} < 0$ so that, in moderately strong acidic solutions, the term $c_{H\oplus}$ in the denominator of Equation 11 can be neglected relative to $K_a^{K\oplus}$. Acid catalysis of enolization saturates for $pH \leq pK_a^{K\oplus}$; a further increase in acid concentration no longer accelerates enolization when the ketone is quantitatively converted to its conjugate acid. However, this saturation is rarely observed at pH values > 0.

In the areas „b“ (pH > 7) and „u“ (pH ≈ 5) the contributions of the base catalyzed and "uncatalyzed" reactions dominate, respectively. The slopes in region "b" are +1 (the rates are proportional to base concentration $c_{OH^\ominus}$ with an apparent coefficient $k_{OH^\ominus}^K = k_0'^K K_a^E/K_w$ for base catalysis), but base catalysis of ketonization saturates at $pH \geq pK_a^E$, when the pre-equilibrium of the enol shifts to the enolate so that k_{obs}^K approaches $k_0'^K$, the first-order rate constant for the protonation of $\mathbf{E}^\ominus$ by water, Equation 6. The pK_a^E values of simple enols are usually around 9–11.

The curves for $\log(k^K/s^{-1})$ and $\log(k^E/s^{-1})$ of acetophenone are parallel in the range $pK_a^{K\oplus} << pH << pK_a^E$ and the vertical distance between them then equals $pK_E = \log(k^K/s^{-1}) - \log(k^E/s^{-1})$. Most ketones are very weak bases, $pK_a^{K\oplus} < 0$, so that the parameter $K_a^{K\oplus}$ does not affect the shape of the pH–rate profiles in the range pH > 1. Base catalysis of ketonization saturates at $pH = pK_a^E$, while the rate of enolization continues to rise, so that the curves for k^E and k^K eventually cross at higher pH. At still higher pH, the rate constant k^E exceeds that of $k^K = k_0'^K$, and k_{obs} follows k^E. The crossing point, for which $k^E = k^K$, lies at $pH = pK_a^K = 18.3$ for acetophenone (Figure 3), which is outside the accessible pH range when ionic strength I is limited to 0.1 M, but pK_a^K is readily calculated from Equation 2.

The rates of ketonization are usually easier to determine (by flash photolysis) than the much slower rates of enolization that require laborious conventional methods such as measuring bromination kinetics and analysis of the reaction products. Thus the shape of the profile is conveniently explored by flash photolysis over a wide range of pH for k^K, and only a single point on the lower curve is then required to determine the enolization constant K_E.

A single reaction path dominates at most pH values, and in these regions the curves are straight lines with slopes of –1, 0, or +1, corresponding to acid catalysis, uncatalyzed reaction, and base catalysis, respectively. The mechanistic implications of positive curvature (increasing slope) and of negative curvature (decreasing slope) differ fundamentally from each other. pH–Rate profiles are readily interpreted with the aid of the following rules.[24]

1. *Positive curvature indicates a change in the reaction mechanism*. In the areas of positive curvature, two reaction paths with different pH-dependence are competitive. The two regions of positive curvature near the bottom of the two

curves in Figure 3 indicate a change from the acid-catalyzed to the uncatalyzed path (around pH 4), and from the uncatalyzed to the base-catalyzed reaction (pH 6).

2. *The same reaction mechanism operates in the regions to the left and right of negative curvature.* In general, negative curvature can arise from two causes: a) Pre-equilibria: As we have seen, acid catalysis of ketone enolization saturates around pH = $pK_a^{K\oplus}$, and base catalysis of enol ketonization saturates around pH = pK_a^{E}. Thus, the acidity constants of reactive intermediates participating in pre-equilibria can be determined by nonlinear least-squares fitting of the kinetic equations to the experimental data. b) A change in the rate-determining step of a reaction can also give rise to negative curvature, when the pH-dependencies of the two steps differ. This case is rarely encountered in keto–enol tautomerization. However, when very low halogen concentrations are used, the second-order reaction of enol trapping does eventually become the rate-determining step of ketone halogenation. Quite accurate enolization constants of some simple ketones have been derived in this way, based on the assumption that halogen trapping is diffusion-controlled, as indicated by the fact that the second-order rate constants of chlorination, bromination, and iodination were found to be nearly the same.[25]

2.5 General Acid and General Base Catalysis

The addition of buffers is required to maintain constant pH during the reaction when experiments are to be carried out in the range 3 < pH < 11. However, keto-enol tautomerization reactions usually exhibit so-called "general" acid and base catalysis.[b,26] The observed rate acceleration with increasing buffer concentration implies that the components of the buffer participate in some rate-determining step of the reaction. In most cases, the rate of reaction increases linearly with increasing buffer concentration at constant buffer ratio, $c_{HB}/c_B^{\ominus}$ = const. (Figure 4a).

[b] "General" acid catalysis is distinguished from "specific" acid catalysis, which applies when a general acid participates only in pre- or post-equilibrium steps; then only the proton concentration $c_{H^\oplus}$ appears in the rate law.

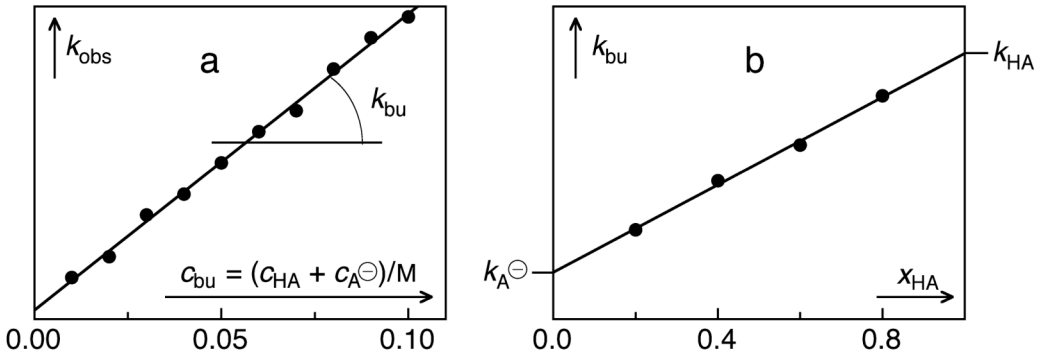

Figure 4. a) Buffer dilution plot; b) Buffer slopes as a function of buffer ratio.

Reaction rate constants applying to wholly aqueous (i.e., unbuffered) solutions are required for pH–rate profiles. These can be obtained by linear extrapolation of a buffer dilution plot to zero buffer concentration. To determine the individual contributions of the general acid and base components of the buffer, the slopes of several dilution series obtained at different buffer ratios are plotted against the mole ratios $x_{HA} = c_{HA}/(c_{HA} + c_{A}^{\ominus})$ of the buffers (Figure 4b). Linear extrapolation to $x_{HA} = 0$ and 1 then gives the catalytic coefficients $k_{A}^{\ominus}$ and k_{HA}, respectively. In general, both coefficients $k_{A}^{\ominus}$ and k_{HA} are found to be different from zero, although they may be difficult to determine accurately, when they are small compared to the rate coefficients of the solvent-derived species.

It may be surprising that the coefficient for general-base catalyzed ketonization, $k_{A}^{\ominus K}$, should differ from zero, because only general acids accelerate the rate-determining steps of ketonization by carbon protonation of **E** and $\mathbf{E}^{\ominus}$. Correspondingly, only general bases accelerate the rate-determining steps of enolization by deprotonation of the ketone or of its conjugate acid. Let's take a look at ketonization, which may occur either by direct protonation of the enol by HA (upper line of Scheme 3) or by pre-equilibrium ionization of the enol, followed by rate-determining carbon protonation of the enolate by HA (lower line).

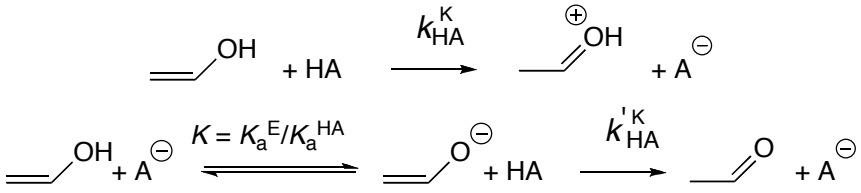

Scheme 3. Rate-determining reactions giving rise to general acid catalysis of ketonization.

Thus, two terms must be added to the rate law of ketonization, Equation 8, and the buffer slopes are given by Equation 15.

$$\left(\frac{\partial k^{K}}{\partial c_{HA}}\right)_{c_{H^{\oplus}}} = \left(k_{HA}^{K} + k'^{K}_{HA}\frac{K_a^E}{c_{H^{\oplus}}}\right)\frac{c_{H^{\oplus}}}{K_a^E + c_{H^{\oplus}}}$$

Equation 15. Buffer slopes for enol ketonization

In the first term, the rate constant k_{HA}^{K} is multiplied by $c_{H\oplus}/(K_a^{E} + c_{H\oplus})$, the fraction of total enol present in neutral form **E**, and in the second term, $k_{HA}'^{K}$ is multiplied by $K_a^{E}/(K_a^{E} + c_{H\oplus})$, the fraction of total enol present in basic form $\mathbf{E}^{\ominus}$ (Equation 4). The observed coefficient for general-base catalysis $k_{A^{\ominus}}^{K}$ is now seen to arise from the pre-equilibrium reaction shown in the second line of Scheme 3. Replacing $(K_a^{E}/c_{H\oplus})c_{HA}$ by $(K_a^{E}/K_a^{HA})c_{A^{\ominus}}$ we find $k_{A^{\ominus}}^{K} = k_{HA}'^{K}K_a^{E}/K_a^{HA}$. Thus, pre-equilibrium deprotonation of the enol by the general base followed by carbon protonation of the ensuing enol anion is operationally equivalent to general base catalysis.

At high buffer concentrations, positive curvature may be observed in buffer dilution plots, indicating that the general acid and base are simultaneously participating in the rate-determining step.[27] In such a case, the rate law must be expanded by third-order terms. Furthermore, plots of buffer slopes versus x_{HB} may be nonlinear, when the unstable tautomer is a diprotic acid as, for example, the *aci*-nitro tautomer of nitrobenzene.[28]

Buffer catalysis has been applied to induce chiral induction by enantioselective protonation; remarkable enantiomeric excess was achieved in the photodeconjugation of α,β-unsaturated ketones and esters by using chiral catalysts for the ketonization of photoenols in aprotic solvents.[29]

3 Examples

The six parameters defining the kinetic and thermodynamic properties of tautomerization reactions that have been determined for a representative selection of carbon acids are collected in Table 1. The column headed by the symbol k_{uc}^{K} contains the observed pH-independent, "uncatalyzed" terms, $k_{uc}^{K} = k_0^{K} + k_{H\oplus}'^{K}K_a^{E}$, of the ketonization rate law (Equation 8). In general, the unprimed symbols k refer to rate constants of the neutral enol tautomer and the primed symbol $k_0'^{K}$ refers to the rate constant for the reaction of enol anion with water (cf. Scheme 2). However, when the stable tautomer is designated as an anion in the left-hand column of Table 1 (e.g., acetoacetate), the unprimed symbols in the header refer to rate or equilibrium constants of the enol anion and the primed symbol $k_0'^{K}$ to the rate constant of the enol dianion. The acidity constants of the neutral ketone, formed by C-protonation of the enol anion, are then listed in the column headed by the symbol $pK_a^{K\oplus}$.

To determine these data, the unstable tautomers were mostly generated by flash photolysis in order to measure their relaxation kinetics in aqueous solution at various pH. Some prototype precursors for the photochemical generation of unstable tautomers are shown in Scheme 4. In a few cases they are formed directly by irradiation of the stable form either by intramolecular photoenolization such as in 2-alkylacetophenones,[30] 2-nitrobenzyl derivatives[28, 31] such as 2-(2',4'-dinitrobenzyl)pyridine,[32] or by light-induced proton transfer to solvent water, as in the case of 9-anthrone.[33]

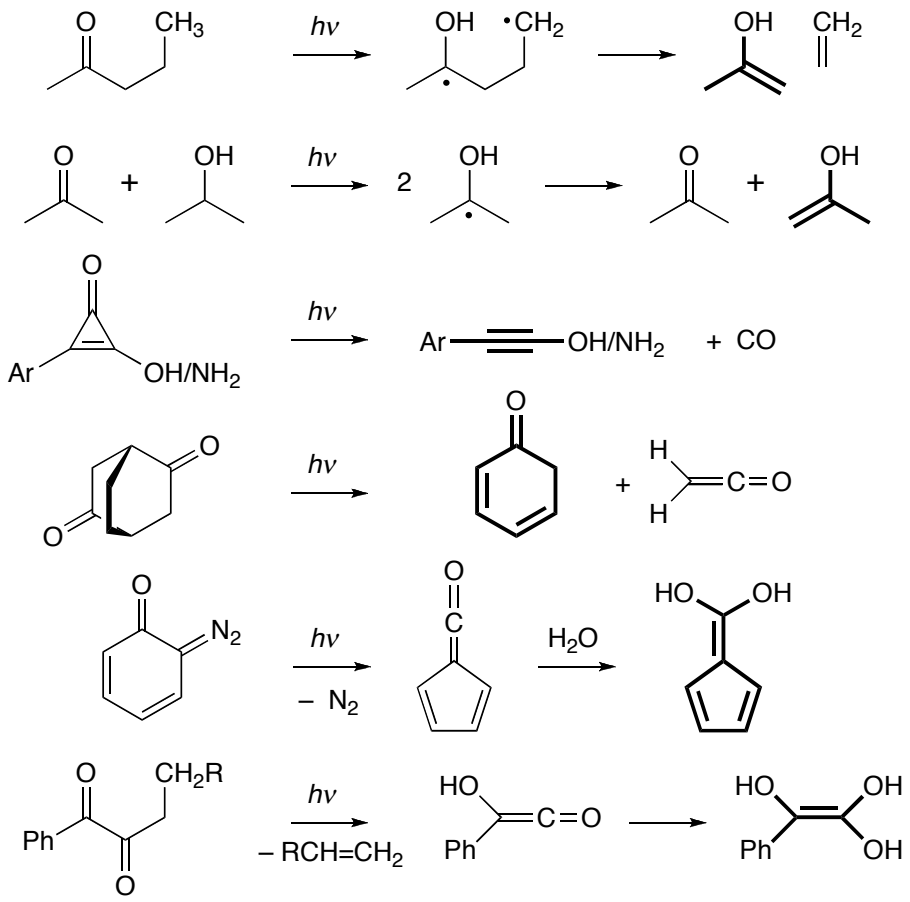

Scheme 4. Prototype reactions used for the generation of unstable tautomers by flash photolysis.

Let us have a look at some instructive pH–rate profiles. That for acetophenone was already discussed in section 2.4 (Figure 3). Its general shape is characteristic for the behaviour of the enols of simple ketones and aldehydes. The enolization constants of aldehydes tend to be higher than those of ketones; compare, for example pK_E(acetone) = 8.33 and pK_E(acetaldehyde) = 6.23. This is in line with the well-known stabilizing effect of alkyl substitution on double bonds, in particular of the polar C=O bond. α-Substitution of ketones and aldehydes by alkyl or, better still, by aryl groups further stabilizes the enol, so that the enol content of 2,2-diphenylacetaldehyde reaches 10%.[34]

The enolization constants of carboxylic acids to form enediols are generally still lower than those of ketones. The pK_E of acetic acid is about 20.[35] Due to the relatively high acidity of 1,1-enediols, the enol content of carboxylate anions is somewhat higher. When the carboxylate is attached to cyclopentadienyl, a strong mesomeric electron acceptor, the conjugate acid of the enol, fulvene-1,1-diol, becomes a strong acid, pK_a = 1.3 and the pK_E of the enol anion is reduced to 5.0.[36-38]

The pH–rate profiles of the enol of 1-indene-3-carboxylic acid and of its ketene precursor, formed from either 1-diazo-2(1*H*)naphthalenone or 2-diazo-1(2*H*)naphthalenone by photochemical deazotization and Wolff-rearrangement,

are shown in Figure 5.[36] The first and second acidity constants of the diol, pK_a^E = 1.9 and $pK_a'^E$ = 8.3, are evident from the downward curvature of $\log(k_{obs}^K/s^{-1})$ at these pH-values. The photo-Wolff rearrangement of diazonaphthoquinones is the active principle of Novolak photoresists.

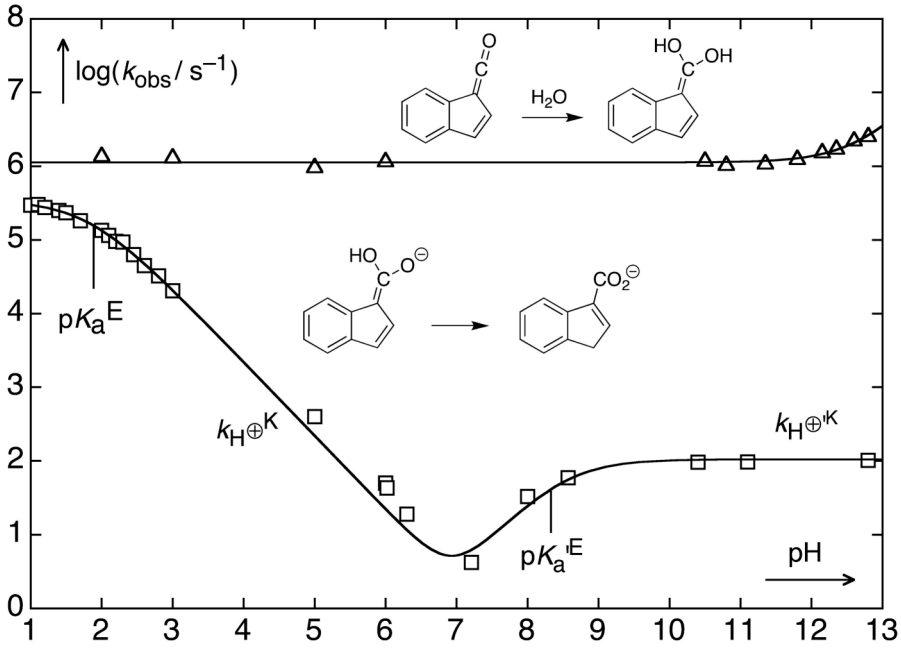

Figure 5. pH–Rate profile of benzofulvene-1,1-diol, the enol of 1-indene-3-carboxylic acid, and its ketene precursor.[36]

Ynols and ynamines are the enol tautomers of ketenes and ketenimines, respectively. They were generated by CO photoelimination from the corresponding cyclopropenones (Scheme 4). Flash photolysis of phenylhydroxycyclopropenone produced transient absorption in the near UV that was monitored at 270 nm and exhibited a biexponential decay.[39, 40] The pH–rate profile and solvent isotope effects served to identify the first of these intermediates as the phenylynolate ion and the second as phenylketene; the identity of the ketene was also confirmed by independent generation through photo-Wolff reaction of benzoyldiazomethane. The kinetic behaviour of phenylynolate is shown in Figure 6. Protonation of the anion to the less reactive neutral phenylynol should produce saturation of acid catalysis. No indication of curvature was seen down to pH 2.8, where the limit in time resolution of the nanosecond apparatus was reached. This sets an upper limit of $pK_a \leq 2.8$ on the acid dissociation constant of phenylynol, which is a remarkable result: it makes phenylynol at least 7 p*K* units more acidic than its double bond analogue, the enol of phenylacetaldehyde, PhCH=CHOH,[41] which, in turn, is some 7 units more acidic than saturated alcohols. With hindsight, such a pK_a difference seems quite reasonable; it is reminiscent of the well-known greater acidity of acetylenic C–H bonds over ethylenic C–H bonds. Both effects may be attributed to charge

delocalization and especially to the increasing s-character and, hence, electronegativity, of carbon with increasing unsaturation.

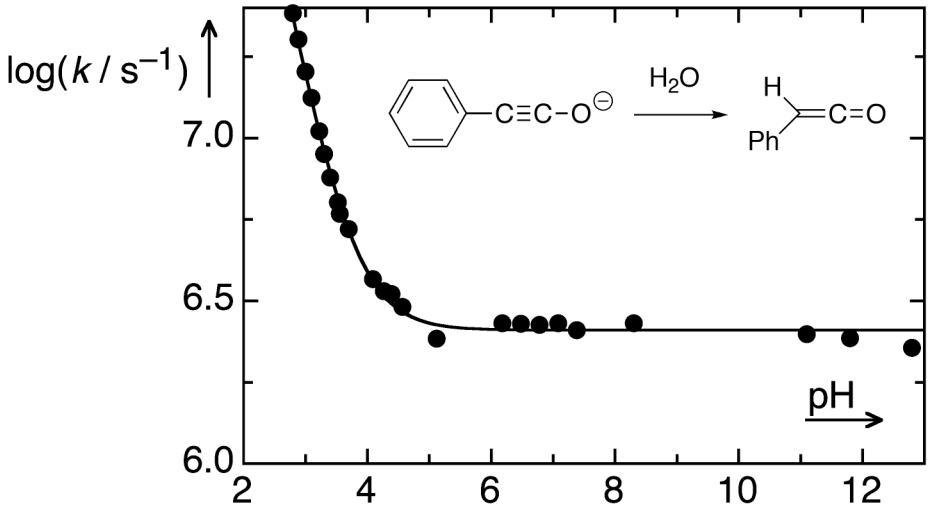

Figure 6. pH–Rate profile for the decay of phenylynol in aqueous solution.[40]

Similarly, ynamines are much stronger acids than enamines and alkylamines.[8, 42-44] Saturation of base catalysis allowed the determination of the NH acidity constant of *N*-(pentafluorophenyl)phenylethynamine in aqueous solution, pK_a^E =10.23.[45]

Aromatic enols, that is, phenols, are generally more stable than their ketone tautomers. The pH–rate profile for the enolization reaction of 2,4-cyclohexadienone to parent phenol is shown in Figure 7.[46] The rate constant k^K of the reverse reaction was determined at pH = 1 by measuring the rate of isotopic exchange and correcting for isotope effects to determine the enolization constant $K_E = k_{H\oplus}^E/k_{H\oplus}^K = 5.4 \times 10^{12}$, $pK_E = -12.73$. The dotted line in the lower part of Figure 7 shows the pH–rate profile of k^K as calculated by Equation 8 using the single value of $k_{H\oplus}^K$ determined at pH = 1. For pH values below pK_a^E = 9.8, where the neutral forms of the ketone and phenol predominate, the two curves are parallel, separated by the distance pK_E. At pH-values above pK_a^E, the phenol ionizes and k^K begins to fall off (slope of –1). This is an unusual case where the addition of base actually *inhibits* the rate of tautomerization! The phenolate is protonated by hydronium ions and the rate increases with acid concentration in the pH-range 11–9. Acid catalysis saturates when phenolate is neutralized at pH < pK_a^E = 9.8, because it is then compensated by the inverse dependence of the phenolate concentration on proton concentration. Above pH 11 the protonation of phenolate by water becomes dominant.

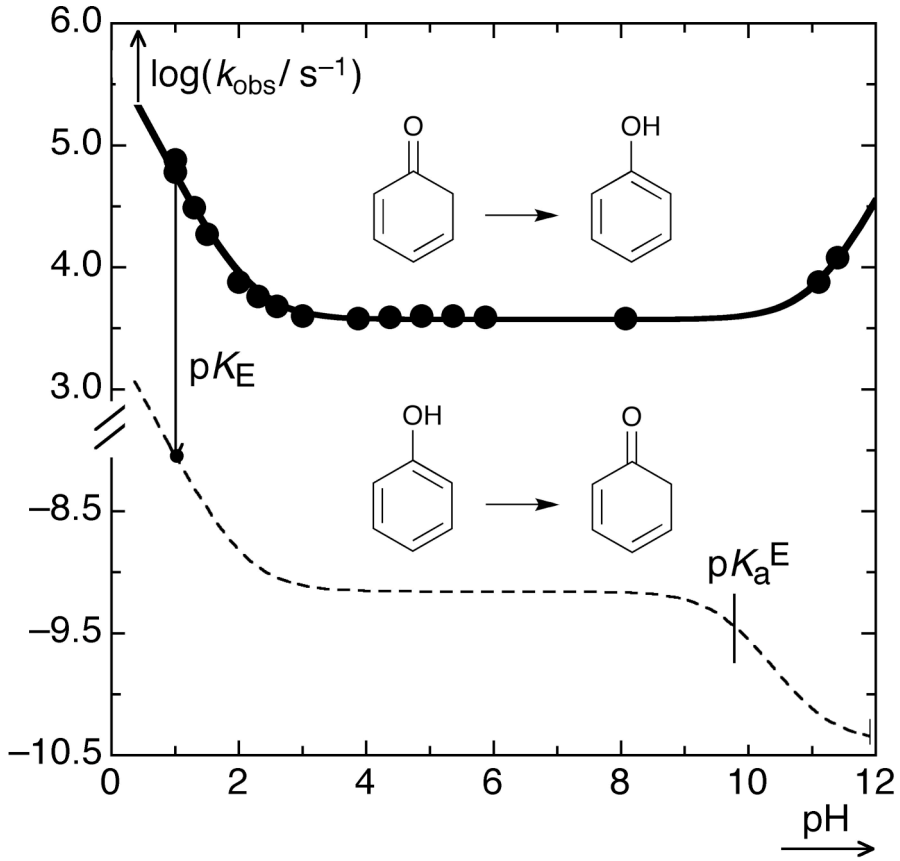

Figure 7. pH–Rate profiles for the enolization of 2,4-cyclohexadienone (upper curve) and for the reverse ketonization reaction (lower curve). Note that ordinate scale is shifted upward by 6.5 units for log(k) values below 3.[46]

The "uncatalyzed" regions of phenol tautomerization cover an unusually wide range from pH 3 to 10. The reason for this dominance of the uncatalyzed reaction, which is barely detectable in the pH–rate profiles of simple ketones (Figure 3) and is absent in carboxylic acids (Figure 5), will become clear from the linear free-energy relationship discussed in section 4.3. The predominant reaction of the ketone in the flat central region is CH-ionization by protonation of water, $k_0^{K} = 3.8 \times 10^3$ s^{-1}. Owing to the large driving force of enolization, the dienone is a remarkably strong carbon acid: $pK_a^{K} = pK_E + pK_a^{E} = -2.9$, which is comparable to the acidity of HCl!

The well-known photochromic tautomerism of 2-(2',4'-dinitrobenzyl)pyridine (CH, Scheme 5) was investigated by flash photolysis in aqueous solution in view of its potential application as a light-activated proton pump.[32] Irradiation of CH yields the enamine tautomer NH (λ_{max} = 520 nm) that rapidly equilibrates with its conjugate base CNO$^-$ (λ_{max} = 420 nm). Transient absorption in the visible region was formed within 30 ns, and decayed by first-order kinetics. The pH–rate profile for the first-order decay rate constant of NH and CNO$^-$, k_{obs}^{in} (Figure 8), determines the acidity constant of NH, $pK_a^{NH} = 5.94$. Rate constants of the reverse reaction k_{obs}^{out} were measured by More O'Ferrall and Quirke[47] using

halogen trapping. Combination with k_{obs}^{in} gave the tautomerization constant $pK_T^{NH} = 8.0$.

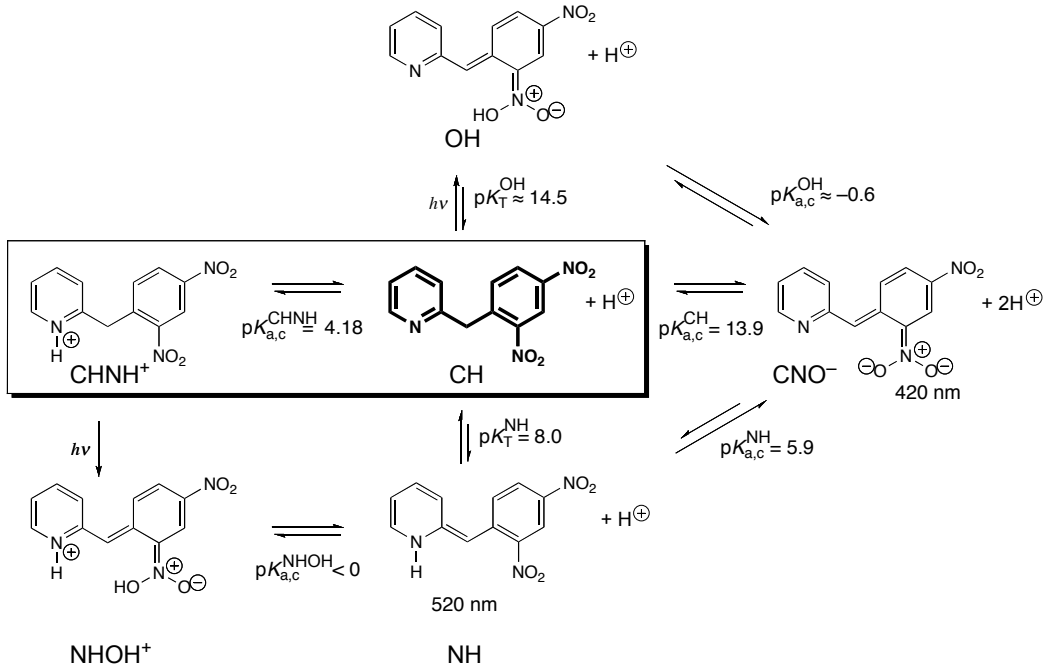

Scheme 5. Tautomerization reactions of 2-(2',4'-dinitrobenzyl)pyridine: A light-activated proton shuttle.[32]

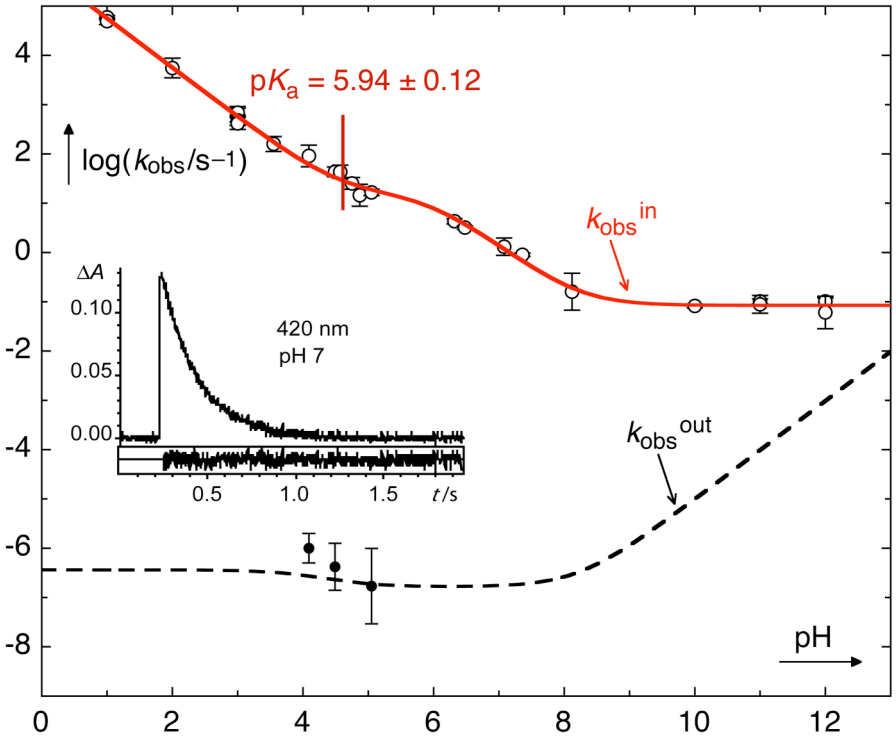

Figure 8. pH–Rate profiles for the decay rate constant k_{obs}^{in} of NH and CNO^- (—) and for the reverse reaction k_{obs}^{in} (– –), see Scheme 5. Reproduced by permission from ref.[32]

Table 1. Kinetic and thermodynamic parameters determined for various tautomeric equilibria in aqueous solution at 25 °C. The symbols for the rate constants k and the equilibrium constants K are explained in the text (first paragraph of section 3). Acidity constants are ionization quotients at ionic strength I = 0.1 M.

stable tautomer	unstable tautomer	pK_E	pK_a^E	p$K_a^{K\oplus}$	$k_{H\oplus}^K$/(M^{-1} s^{-1})	k_{uc}^K/s^{-1}	$k_0'^K$/s^{-1}	Ref.[a]
acetone	propen-2-ol	8.33	10.94	–3.06	5.38×10^3	0.077	5.0×10^4	20, 48, 49
butan-2-one	2-buten-2-ol	7.51		–3.48	839			50, 51
butan-2-one	1-buten-2-ol	8.76		–3.48	6.30×10^3			50, 51
3-methylbutan-2-one	3-methyl-1-buten-2-ol	8.60		–3.63	5.93×10^3			50, 51
3-methylbutan-2-one	3-methyl-2-buten-2-ol	7.33		–3.63	233			50, 51
3,3-dimethylbutan-2-one	3,3-dimethyl-1-buten-2-ol	8.76		–3.48	7.51×10^3			50, 51
pentan-3-one	2-penten-3-ol	7.43		–3.88	793			50, 51
cyclopentanone	cyclopenten-1-ol	7.94			5.3×10^3			50, 51
cyclohexanone	cyclohexen-1-ol	6.38	11.7		577			50, 51
cycloheptanone	cyclohepten-1-ol	8.00			4.0×10^3			50, 51
2,4-dimethylpentan-3-one	2,4-dimethylpent-1-en-3-ol	7.52			97.5			50, 51
acetophenone	α-hydroxystyrene	7.96	10.35	–3.87	1.25×10^3	0.18	7.2×10^3	4, 20-23
isobutyrophenone	1-phenylisobuten-1-ol	6.48	11.78		2.14	5.1×10^{-4}	69	52
1-tetralone	3,4*H*-naphthalen-1-ol	7.31	10.82		180	1.1×10^{-2}	743	53
1-indanone	indene-3-ol	7.48	9.48		904	0.26	501	54
2-indanone	indene-2-ol	3.84	8.36		3.36	0.207	6.95	55
isochroman-4-one	1*H*-2-benzopyran-4-ol	5.26	10.13		0.090		10.8	53
acetoacetate	acetoacetate enol	2.91	13.18		1.28×10^5	1.8×10^{-2}	9.06×10^2	56
4,4,4-trifluoroacetoacetate	trifluoroacetoacetate enol	0.61	9.95		7.44×10^2	2.12×10^{-3}	3.2×10^{-2}	57
oxocyclohexane-2-CO_2^-	cyclohexen-1-ol-2-CO_2^-	1.99	14.53		1.35×10^4	2.32×10^{-5}	18.0	58
oxocyclopentane-2-CO_2^-	cyclopenten-1-ol-2-CO_2^-	3.00	12.41		2.41×10^5	2.57×10^{-2}	484	59
3,3,5,5-tetramethyl-oxocyclopentane-2-CO_2^-	3,3,5,5-tetramethyl cyclopenten-1-ol-2-CO_2^-	1.83	14.4		7.60×10^4	1.74×10^{-3}	310	60
oxocyclobutane-2-CO_2^-	cyclobuten-1-ol-2-CO_2^-	5.97	8.47		1.59×10^7	12.8	319	61
phenol	cyclohexa-2,4-dienone	–12.73	9.84		1.0×10^{-7}	7.1×10^{-10}	4.1×10^{-11}	46
phenol	cyclohexa-2,5-dienone	–11.0	9.84		3.0×10^{-7}	8.4×10^{-10}		46

1-naphthol	benzo[*b*]cyclohexa-2,5-dienone	–6.2	9.25		5.7×10^{-5}	1.3×10^{-7}	1.0×10^{-7}	62
1-naphthol	benzo[*b*]cyclohexa-2,4-dienone	–7.1	9.25		2.8×10^{-5}	5.7×10^{-7}	7.8×10^{-8}	62
9-anthrone	9-anthrol	2.14	7.84		0.032	1.8×10^{-3}	8.3×10^{-3}	33, 63
acetaldehyde	vinyl alcohol	6.23	10.50		33	0.039	882	64
isobutyraldehyde	2-methylpropen-1-ol	3.86	11.63		0.59	4.0×10^{-4}	6.6	65
2-phenylacetaldehyde	*cis*-2-phenylethen-1-ol	3.35	9.76		0.190		4.1	41
2-phenylacetaldehyde	*trans*-2-phenylethen-1-ol	3.07	9.46		0.0745		1.33	41
2,2-diphenylacetaldehyde	2,2-diphenylethen-1-ol	0.98	9.40		2.1×10^{-3}	7.0×10^{-4}	0.106	34
cyclopentadienyl-1-CO_2H	fulvenediol	8.4	1.31			1.1×10^{8}		36-38
cyclopentadienyl-1-CO_2^-	fulvenediol anion	5.0	8.7	4.71	2.2×10^{7}		3	36-38
1-indene-3-carboxylic acid	benzofulvenediol	9.3	1.90			2.8×10^{5}		36
1-indene-3-carboxylate	benzofulvenediol anion	6.6	8.3	4.50	2.21×10^{7}		105	36
fluorene-9-carboxylic acid	dibenzofulvenediol	9.67	2.01			1.23×10^{6}		66
fluorene-9-carboxylate	dibenzofulvenediol anion	8.24	9.61	11.67	1.25×10^{8}	30	3.22×10^{3}	66
phenylcyanoacetate	α-cyano-β,β-diHOstyrene anion	6.49	8.70	8.22	2.09×10^{7}		2.53×10^{4}	67
mandelic acid	α,β,β-trihydroxystyrene	16.19	6.39		9.03×10^{3}	3.89×10^{2}	1.7×10^{5}	68, 69
methyl mandelate	α,β-dihydroxy-β-MeOstyrene		6.55			5.24×10^{2}	4.20×10^{5}	70
mandelamide	β-amino-α,β-dihydroxystyrene	15.88	8.40		1.7×10^{6}		2.56×10^{6}	71
diisobutenyl ketone (phorone)	2,6-Me_2-4-OH-1,3,5-heptatriene	7.2	10.84		200	2.6	378	72
phenylketene	phenylethynol		≤2.8			$\geq2\times10^{7}$ [b]	2.52×10^{6}	39, 40
phenylketenimine	phenylethynamine		≤18 [c]					42
N-(C_6F_5)-phenylketenimine	*N*-(C_6F_5)-phenylethynamine		10.23		8.9×10^{2}	1.08	6.52×10^{5}	45
1*H*-indole	3*H*-indole	5.8			4.9×10^{6}	0.207		73
2-(2',4'-dinitrobenzyl)pyridine	enamine tautomer	8.0	5.94		5.8×10^{5}	17	0.09	32, 47
2-nitrotoluene	*aci*-nitro tautomer	17	3.57		1.3×10^{5}		1.16	31

[a] The $pK_a^{K\oplus}$ values of protonated ketones were taken from ref.[19] [b] Calculated from the observed rate constant $k_{H\oplus}{}'^{K} = 1.34\times10^{9}$ M^{-1} s^{-1}, Equation 18. [c] Calculated from the observed rate constant $k_{OH}{}^{K} = k_0{}'^{K}K_a{}^{E}/K_w = 6.5\times10^{6}$ M^{-1} s^{-1} assuming $k_0{}'^{K} \leq 1\times10^{11}$ s^{-1}.

4 Rate–Equilibrium Relationships

4.1 The Brønsted Relation, Statistical Factors, and the Acidity of Solvent-Derived Species ($H^{\oplus}$ and H_2O)

Keto–enol tautomerization reactions usually exhibit general acid and general base catalysis (section 2.5). The rate coefficients for general acid catalysis, k_{HA}, determined from a series of buffer dilution plots (Figure 4) tend to obey a linear log–log relationship to the acidity constants K_a^{HA} of the catalysts. Similarly, the coefficients of general base catalysis $k_{A^{\ominus}}$ are related to the basicity constants $K_b^{A} = K_w/K_a^{HA}$ of the buffer bases, as was first reported by Brønsted and Pedersen in 1924.[74] Taking account of the appropriate statistical factors p and q,[75, 76] the Brønsted relations may be written as in Equation 16.[77, 78]

$$\log\left(\frac{k_{HA}}{p}\right) = \log G_A + \alpha \log\left(\frac{qK_a^{HA}}{p}\right)$$

$$\log\left(\frac{k_{A^{\ominus}}}{q}\right) = \log G_B + \beta \log\left(\frac{pK_b^{A}}{q}\right) = \log G_B + \beta \log\left(\frac{pK_w}{qK_a^{HA}}\right)$$

Equation 16. The Brønsted relations for general acid and base catalysis.

The factor p is equal to the number of equivalent acidic hydrogens in a given general acid HA and the factor q represents the number of equivalent sites for proton attachment at the conjugate base $A^{\ominus}$, G_A and G_A are constants for a given reaction, and the Brønsted parameters α and β are considered to be constant for a series of buffers with varying acidity or basicity. A plot of $\log(k_{HA}/p)$ versus $\log(qK_a^{HA}/p)$ should therefore be linear with a slope of α. This hypothesis has been amply confirmed. Equation 16 represent a linear free energy relationship for general acid and base catalysis, because $2.3RT\mathrm{p}K_a^{HA}$ is equal to the free energy of ionization of the general acid HA.

Rate theories generally require rate–equilibrium relationships to be curved rather than linear (see section 4.2). Brønsted and Pedersen already noted that the bimolecular rate coefficients $k_{A^{\ominus}}$ cannot increase indefinitely with increasing base strength of the catalyst, because they will eventually be limited by the rate of diffusion. Slight variation of the slope α becomes perceptible when a wide range of general acids is used.[20, 52] The variation of α becomes quite evident when general acid or base catalysis is compared for substrates with widely different free energies of reaction. Brønsted slopes α, determined in each case with a series of general acids, vs. the free energies $\Delta_r G°$ for C-protonation of enols or enolates are given in Table 2 and plotted in Figure 9. To determine $\Delta_r G°$, the acidity constants of the general acids used in the corresponding Brønsted plots were averaged.

Table 2. Brønsted parameters α and average reaction free energies $\Delta_r G°$ of the reactions **E** + HA $\rightarrow$ $\mathbf{K}^{\oplus}$ + $A^{\ominus}$ and $\mathbf{E}^{\ominus}$ + HA $\rightarrow$ **K** + $A^{\ominus}$.

enol, enolate	α	$\Delta_r G°$/(kJ mol^{-1}) [a]	α_{calc} [b]	ref.
acetophenone enolate	0.32	–83.5	0.31	20
isobutyrophenone enolate	0.37	–83.3	0.31	52
1-naphtholate – 4*H*-naphthone	0.62	0.0	0.50	62, 79
phenylynolate	0.25	–109.0	0.25	40
phenolate – 2,4-cyclohexadienone	0.67	52.7	0.62	46
isochroman-4-one enolate	0.47	–47.9	0.39	53
9-anthrolate	0.56	–26.3	0.44	33
mandelamide enolate	0.31	–97.1	0.28	71
acetophenone enol	0.50	–0.7	0.49	20
isobutyrophenone enol	0.58	6.8[c]	0.52	52
1-naphthol – 4*H*-naphthone	0.85	77.0[d]	0.67	62, 79

[a] Calculated from the data given in Table 1. [b] Calculated using Equation 20. [c] $pK_a^{K\oplus} = -3.9$ was assumed. [d] $pK_a^{K\oplus} = -3.6$ was assumed.

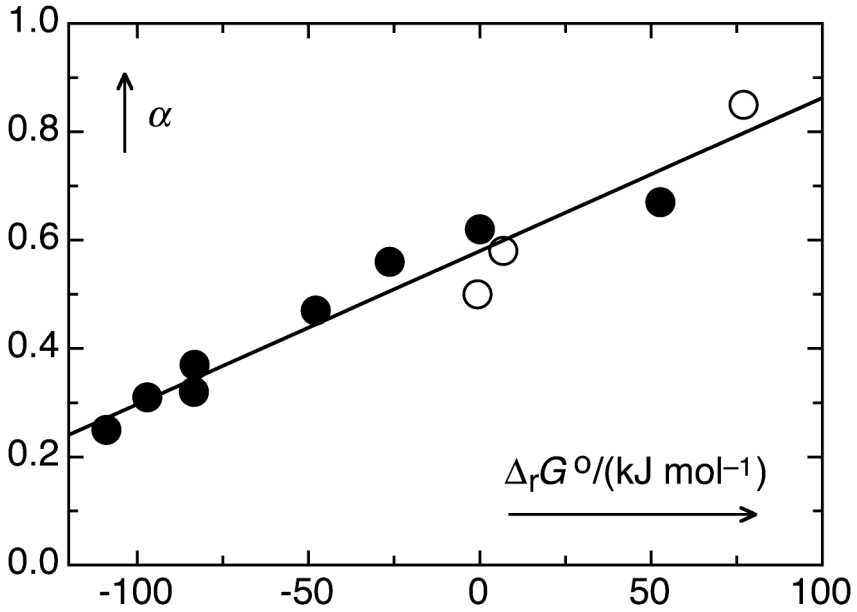

Figure 9. Variation of the Brønsted parameter α for general acid catalysis of enol ketonization with the free energy change $\Delta G°$ for carbon protonation of enols (o) and enolates (•). The data are taken from Table 2.

The Brønsted exponent α increases from about 0.2 for strongly exergonic reactions (C-protonation of phenylethynolate) to ≈ 0.8 for strongly endergonic reactions (protonation of 1-naphthol at carbon atom 4). The observed increase of the Brønsted slope with increasing free energy of reaction is an exemplification of the Hammond postulate, because the Brønsted parameter α may be regarded as a measure of the extent of proton transfer in the transition state: highly exergonic reactions have an early transition state ($\alpha \rightarrow 0$), endergonic reactions

have a late transition state ($\alpha \rightarrow 1$). The empirical correlation of the parameters α with the reaction free energies $\Delta_r G°$ shown in Figure 9 will be recast in terms of the Marcus model of proton transfer at the end of section 4.3.

If one includes the solvent-derived acids $H^{\oplus}$ and H_2O in a Brønsted plot, they often deviate substantially from the regression line of general acids. The rate constants predicted from the regression tend to be larger than the observed values. What is the reason for these discrepancies? To begin with, it should be mentioned that the "pK_a" values of the proton and of water are 0 (by definition) and about 14.0 (i.e., equal to pK_w) and not –1.74 and 15.74, as is erroneously stated in most textbooks of organic chemistry. The latter values originate from the inclusion of the concentration c_{H_2O} = 55.5 M, log(55.5) = 1.74, in the equilibrium constants corresponding to reaction equations such as Equation 17.

$$H_2O \rightarrow H^{\oplus} + HO^{\ominus}$$

Equation 17. Auto-ionization of water

The derivation of the law of mass action from the second law of thermodynamics defines equilibrium constants $K°$ in terms of activities. For dilute solutions and low ionic strengths, the numerical values of the molar concentration quotients of the solutes, if necessary amended by activity coefficients, are acceptable approximations to $K°$ (Equation 3). However, there exists no justification for using the numerical value of a solvent's molar concentration as an approximation for the pure solvent's activity, which is unity by definition.[80, 81]

Thus, firstly, the choice of the pure solvent as the reference state for the definition of activities of solutes in fact impairs a fair comparison of the activity of dilute solutes such as general acids to the activity of the solvent itself. Secondly, the observed first-order rate constants k_0 or k_0' for the reaction of a solute with the solvent water are usually converted to second-order rate constants by division through the concentration of water, $k_{H_2O} = k_0/c_{H_2O}$, for a comparison with the second-order rate coefficients k_{HA}. Again, it is questionable whether the formal k_{H_2O} coefficients so calculated may be compared with truly bimolecular rate constants k_{HA} for the reactions with dilute general acids HA. It is then no surprise that the values for the rate coefficients determined for the catalytic activity of solvent-derived acids scatter rather widely, often by one or two orders of magnitude, from the regression lines of general acids.[77]

Hydronium ion catalytic coefficients for enolization and ketonization of simple aldehydes and ketones correlate with the enolization equilibrium constants pK_E.[50] The slopes of the two correlations are of opposite sign (–0.17 and 0.83, respectively), ketonization being considerably more sensitive to a change in the driving force.

4.2 Mechanism of the "Uncatalyzed" Reaction

pH–Rate profiles frequently exhibit a more or less pronounced flat portion at pH-values near neutral, where tautomerization is catalyzed neither by acid nor by base. In the case of phenol (Figure 7), the "uncatalyzed" reaction dominates in the range of $4 \leq pH \leq 10$. Several kinetically indistinguishable, pH-independent mechanisms may be considered as pathways of tautomerization. Facile intramolecular 1,5-H shifts are observed in the ketonization of 1,3-dienols (see, e.g., the entry phorone in Table 1). Intramolecular 1,3-H shifts, on the other hand, are ruled out on the basis of the prohibitively high activation energies that are unanimously predicted by calculations. Indeed, enols are kinetically stable in dry solvents or in the gas phase. Clearly, the solvent participates in these reactions. Water being amphoteric, it might intervene (a) as a general acid, (b) as a general base, or (c) by promoting a "concerted" transfer of two protons through a bridge of one or more water molecules (Scheme 6).

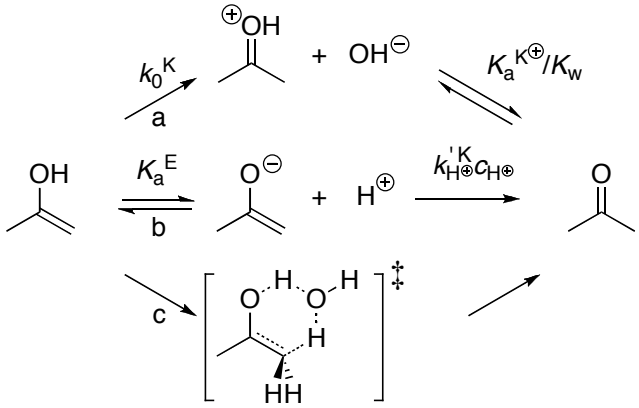

Scheme 6. Reaction paths considered for the "uncatalyzed" term k_{uc}^K.

Rate constants of ketonization of acetophenone enol along paths (a) and (b) have been be estimated using the Brønsted Equation 16.[20] Those predicted for path (a) are orders of magnitude below the observed rate constant $k_{uc}^K = 0.18\ s^{-1}$, while those for path (b) were found to be in reasonable agreement with experiment. The concerted mechanism (c) does not satisfactorily account for structure-reactivity relationships observed in aqueous solution. It may, however, well be the dominant mechanism in aprotic solvents containing small amounts of water. In the next section we will show that for most compounds, the pH-independent terms $k_{uc}^K = k_0^K + k_{H⊕}'^K K_a^E$ (Equation 8) determined in aqueous solution can be attributed to water reacting as a general base, path (b), that corresponds to the second term, where $k_{H⊕}'^K$ is the rate constant for proton addition to $\mathbf{E}^⊖$.

$$k_{uc} \approx k_{H⊕}'^K K_a^E$$

Equation 18.

Ketonization along path (b) liberates a proton in the pre-equilibrium step and the proton is removed by subsequent protonation of $\mathbf{E}^⊖$. While the rate of the second, rate-determining step is directly proportional to the concentrations $c_{E^⊖}$

and $c_{H\oplus}$, the concentration $c_E{}^{\ominus}$ is itself inversely proportional to $c_{H\oplus}$ as long as $c_{H\oplus} >> K_a^E$ (Equation 4), so that the overall contribution of this path to the overall rate of reaction is pH-independent.

4.3 The Marcus Model of Proton Transfer

The experimental ketonization rate constants k^K collected in Table 1 cover a range of twenty orders of magnitude. A logarithmic plot against the corresponding reaction free energies $\Delta_r G°$ reveals that these data follow a systematic, nonlinear trend, Figure 10.

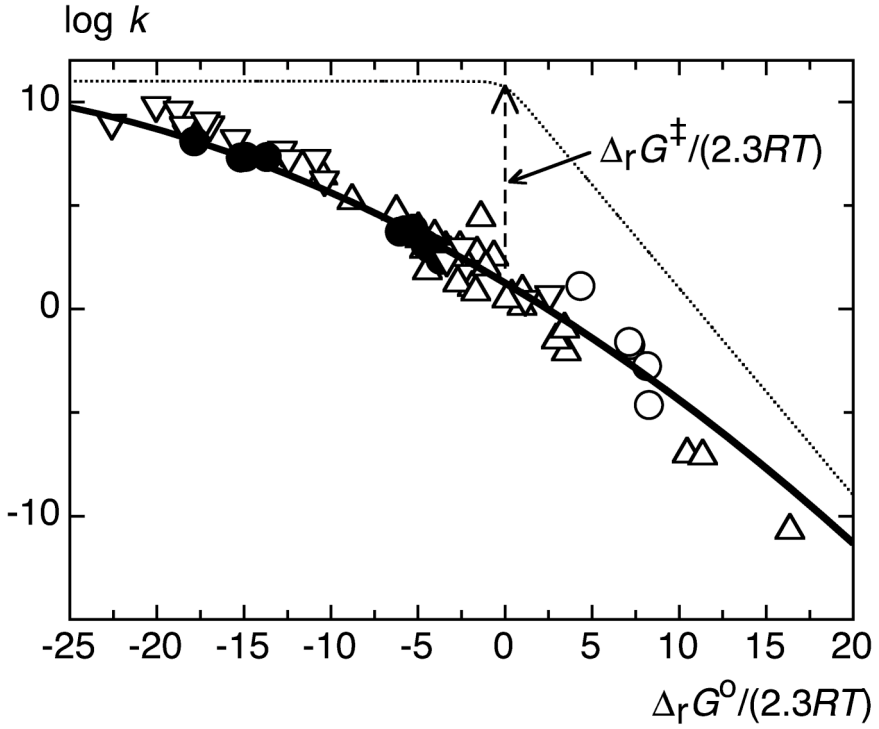

Figure 10. Empirical relationship between the logarithm of the proton transfer rate constants (Table 1) and the corresponding free energies of reaction $\Delta_r G°$. Triangles (∇): $k_{H\oplus}{}'^K/(M^{-1}\ s^{-1})$. Filled circles (●): $k_{H\oplus}{}^K/(M^{-1}\ s^{-1})$. Empty circles (O): $k_0{}^K/s^{-1}$. Triangles (Δ): $k_0{}'^K/s^{-1}$. The solid line was obtained by fitting of the Marcus Equation 19.

The free energy of reaction associated with a given rate constant is determined by the equilibrium constant of that reaction. Thus, for the reaction $\mathbf{E} + H^{\oplus} \rightarrow \mathbf{K}^{\oplus}$ ($k_{H\oplus}{}^K$, filled circles •, centre), we have $\Delta_r G° = -2.3RT(pK_E + pK_a{}^{K\oplus})$]; for the reaction $\mathbf{E}^{\ominus} + H^{\oplus} \rightarrow \mathbf{K}$ ($k_{H\oplus}{}'^K$, triangles ∇, upper left), $\Delta_r G° = -2.3RT(pK_E + pK_a{}^E)$; for the protonation of enolates by water, $\mathbf{E}^{\ominus} + H_2O \rightarrow \mathbf{K} + HO^{\ominus}$ ($k_0{}'^K$, triangles Δ, lower right), $\Delta_r G° = -2.3RT(pK_E + pK_a{}^E - pK_w)$; finally, for the reaction of enols with water, $\mathbf{E} + H_2O \rightarrow \mathbf{K}^{\oplus} + HO^{\ominus}$ ($k_0{}^K$, empty circles ○, lower right), $\Delta_r G° = -2.3RT(pK_E + pK_a{}^K - pK_w)$. Statistical factors (section 4.1) were taken into account, i.e., the rate constants were divided by the number of equivalent basic carbon atoms of the enol (e.g., q = 1 for acetone enol and q =

2 for phenol reacting to cyclohexa-2,5-dienone) and the free energy terms $\Delta_r G°/(2.3RT)$ were corrected by –log(p/q), where p is the number of equivalent acidic protons in the ketone (e.g., p = 6 for acetone). These corrections are small compared to the variation of the rate constants.

The dotted line shown in the upper part of Figure 10 represents the free-energy relationship expected for "normal" bases, in which the nucleophilic centre is an O or N heteroatom ("Eigen"-curve[82]); exergonic reactions are diffusion-controlled ($k_d \approx 10^{11}$ M^{-1} s^{-1}) and the rates of endergonic reactions decrease with a slope of –1 vs. $\Delta_r G°/(2.3RT)$. The rate constants of the carbon bases ("pseudo"-bases) studied here are much lower than predicted by the Eigen-curve, particularly in the region around $\Delta_r G° = 0$, where the difference amounts to some ten orders of magnitude. The systematic trend of the rate data shown in Figure 10 is reasonably well captured by the Marcus expression for proton transfer,[83] which takes the simple form of Equation 19 when work terms are omitted.[84]

$$\log\frac{k}{k_d} = \left(\frac{-\Delta_r G^{‡}}{\ln(10)RT}\right), \text{ where } \Delta_r G^{‡} = \Delta_r G_0^{‡}\left(1+\frac{\Delta_r G^{o}}{4\Delta_r G_0^{‡}}\right)^2$$

Equation 19. Marcus' expression for proton transfer

The parameter $\Delta_r G_0^{‡}$ is called the "intrinsic" barrier, the barrier of a thermoneutral reaction, $\Delta_r G° = 0$. The rate of diffusion was assumed as $k_d = 1 \times 10^{11}$ M^{-1} s^{-1}. Nonlinear least-squares fitting of Equation 19 to the set of data gave $\Delta_r G_0^{‡} = 55.6 \pm 0.7$ kJ mol^{-1}. In an earlier treatment using a smaller set of data we had obtained $\Delta_r G_0^{‡} = 57 \pm 2$ kJ mol^{-1}.[7]

In most cases, the rate constants k_{uc}^{K} were converted to $k_H⊕'^{K}$ (Equation 18) assuming that mechanism (b) of Scheme 6 accounts for the uncatalyzed reaction. Clearly, the rate constant k_{uc}^{K} for phorone should not be converted to $k_H⊕'^{K}$, because the uncatalyzed reaction is due to an intramolecular 1,5-H shift rather than to pre-equilibrium ionization of the enol. Conversion of $k_0^{K} = 2.6$ s^{-1} would give $k_H⊕'^{K} = 1.8 \times 10^{11}$ M^{-1} s^{-1}, which is higher than any of the values observed for simple enols and more than two orders of magnitude higher than that predicted by the Marcus equation for $k_H⊕'^{K}$.

Similar arguments apply to the six α-carboxy-substituted ketones that have been studied by Kresge and coworkers (entries acetoacetate to oxocyclobutane-2-carboxylate in Table 1). Kresge already noted that the rate constants k_{uc}^{K} observed for the "uncatalyzed" ketonization of some of these compounds would give unrealistically high calculated values for $k_H⊕'^{K}$ near or above 10^{11} M^{-1} s^{-1} using Equation 18. Indeed, these calculated values of $k_H⊕'^{K}$ are about two orders of magnitude above those expected from the Marcus relation except that for 4,4,4-trifluoroacetate. The rate constants k_{uc}^{K} observed for the formation of these α-carboxy-substituted ketones are, however, close to those expected for the protonation of the neutral enols by water, $k_{uc}^{K} = k_0^{K}$.

The modest amount of scatter in Figure 10 is remarkable, considering that it includes four different reaction types (carbon protonation of enols or enolates by hydronium ions or by water) and a wide range of substrates. The standard deviation between the 62 observed values of $\log k^{K}$ and those calculated by Equation 19 is 0.95.

The acidity constants of protonated ketones, $pK_a^{K\oplus}$, are needed to determine the free energy of reaction associated with the rate constants $k_{H\oplus}^{K}$, $\Delta_r G° = -2.3RT(pK_E + pK_a^{K\oplus})$. Most ketones are very weak bases, $pK_a^{K\oplus} < 0$, so that the acidity constant $K_a^{K\oplus}$ cannot be determined from the pH–rate profile in the range $1 < pH < 13$ (see Equation 11 and Figure 3). The acidity constants $K_a^{K\oplus}$ of a few simple ketones were determined in highly concentrated acid solutions.[19] Also, carbon protonation of the enols of carboxylates listed in Table 1 (entries cyclopentadienyl 1-carboxylate to phenylcyanoacetate) give the neutral carboxylic acids, the carbon acidities of which are known and are listed in the column headed $pK_a^{K\oplus}$. As can be seen from Figure 10, the observed rate constants $k_{H\oplus}^{K}$ for carbon protonation of these enols (8 data points marked by the symbol • in Figure 10) accurately follow the overall relationship that is defined mostly by the data points for $k_{H\oplus}^{'K}$ and $k_0^{'K}$. We can thus reverse the process by *assuming* that the Marcus relationship determined above holds for the protonation of enols and use the experimental rate constants $k_{H\oplus}^{K}$ to estimate the acidity constants $K_a^{K\oplus}$ of ketones via the fitted Marcus relation, Equation 19. This procedure indicates, for example, that protonated 2,4-cyclohexadienone is less acidic than simple oxygen-protonated ketones, $pK_a^{K\oplus} = -1.3$.

Marcus' rate theory is useful to rationalize the connection between reactivity and the slope α of Brønsted plots. The derivative of Equation 19 with respect to $\Delta_r G°$ is the slope of the Marcus curve, which corresponds to the Brønsted exponent α for a given free energy of reaction $\Delta_r G°$, Equation 20.[77, 84]

$$\alpha = \left(\frac{\partial \Delta_r G^{\ddagger}}{\partial \Delta_r G^{o}} \right)_{p,T} = \left(1 + \frac{\Delta_r G^{o}}{4 \Delta_r G_0^{\ddagger}} \right) / 2$$

Equation 20

The Brønsted parameter α varies substantially over the large range of $\Delta_r G°$ covered by the experimental data collected in Figure 10; it ranges from 0.2 for the most reactive enolates (phenylethynol anion) to about 0.8 for the least reactive compound (1-naphthol). The α-values calculated by Equation 20 are in satisfactory agreement with those determined experimentally from Brønsted plots of general acid catalysis (Table 2).

The second derivative of Equation 19 with respect to $\Delta_r G°$, Equation 21, represents the change of α with increasing $\Delta_r G°$. Using the fitted value of $\Delta_r G_0^{\ddagger} = 55.6$ kJ mol^{-1}, one obtains $\partial\alpha/\partial\Delta_r G° = 0.22 \times 10^{-3}$ mol kJ^{-1}. The slope of Figure 9 amounts to 0.28×10^{-3} mol kJ^{-1}.

$$\left(\frac{\partial^2 \Delta_r G^{\ddagger}}{\partial\left[\Delta_r G^{o}\right]^2}\right)_{p,T} = \left(\frac{\partial \alpha}{\partial \Delta_r G^{o}}\right)_{p,T} = \frac{1}{8\Delta_r G_0^{\ddagger}}$$

Equation 21

Using these relations, the rate coefficients for specific and general acid catalysis, $k_{H}\oplus$ and k_{HA}, of any keto-enol tautomeric reaction can be predicted from the appropriate free energy of reaction $\Delta_r G°$. The required thermochemical data can be estimated using group additivity rules[85, 86] or quantum chemical calculations. Equation 20 also rationalizes the fact that the "uncatalyzed", pH-independent portion of pH–rate profiles is marginal for ketones and absent for carboxylic acids with low enol content ($\alpha \rightarrow 0$), but dominates the pH-profile of phenol ($\alpha \rightarrow 1$). The pH-independent contribution is generally due to the reaction $\mathbf{E}^{\ominus} + H^{\oplus} \rightarrow \mathbf{K}$, which corresponds to the most exergonic reaction. The corresponding rate constants $k_{H}\oplus'^{K}$ are approaching the limit of diffusion control for simple ketones and are therefore much less sensitive to changes in $\Delta_r G°$ than the acid- and base-catalyzed branches of the pH-profiles due to $k_{H}\oplus^{K}$ and $k_0'^{K}$. As an example, the pH–rate profiles for the ketonization of phenol and acetophenone enol are shown in Figure 11 (thick lines), together with the contributions of the three individual terms of Equation 9 (dotted lines: $k_{uc}^{K} = k_{H}\oplus'^{K} K_a^{E}$; dashed lines: $k_{H}\oplus^{K}$; long dashed lines: $k_0'^{K}$). Clearly, the uncatalyzed term that is due to the fastest rate constant $k_{H}\oplus'^{K}$ increases less than the others when going to the much more exergonic ketonization of acetophenone enol, so that it is marginalized.

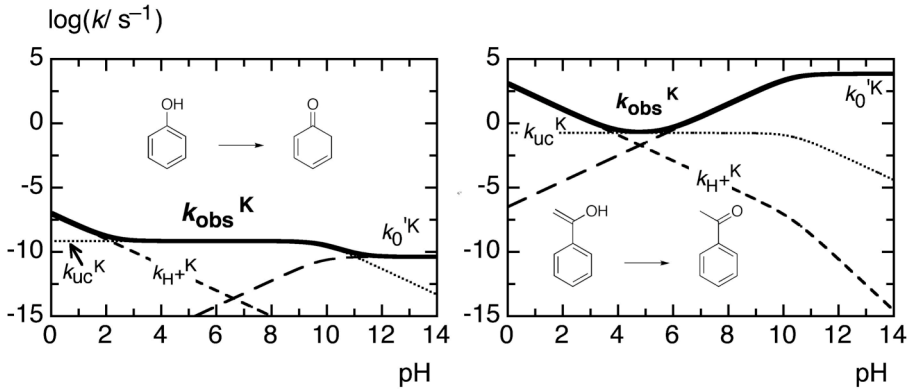

Figure 11. Effect of Brønsted-α on the shape of the pH–rate profile of ketonization.

The extended pH-independent branch seen in the pH-profile of phenylynol (Figure 6) has an entirely different origin: due to the high acidity of the ynol, $pK_a^{E} < 2.7$, the ynol anion is predominant over the whole observable pH range, and the pH-independent process observed above pH 5 is its protonation by solvent water, $\mathbf{E}^{\ominus} \rightarrow \mathbf{K} + HO^{\ominus}$.

5 Conclusion and Outlook

Flash photolysis has provided a wealth of kinetic and thermodynamic data for tautomerization reactions. Equilibrium constants of enolization, K_E, spanning a range of 30 orders of magnitude, have thereby been determined accurately as the ratio of the rate constants of enolization, k^E, and of ketonization, k^K. Nowadays, tautomerization constants K_E can be predicted with useful accuracy by performing *ab initio* or density functional theory calculations. Free energy relationships based on empirical data can then be used to estimate the lifetime of unstable tautomers in wholly aqueous solutions and in aqueous buffers. These studies have uncovered some remarkable findings such as the CH-acidity of 2,4-cyclohexadienone, $pK_a^E = -2.9$, or the unusually high acidities of ethynols and ethynamines. The analysis of these data provides reliable assignments for the elementary reactions that govern tautomerization reactions and how they depend on pH.

6 References

1. Erlenmeyer, E., *Chem. Ber.* **1880**, *13*, 305.
2. Lapworth, A., *J. Chem. Soc.* **1904**, *85*, 30-42.
3. Hochstrasser, R.; Kresge, A. J.; Schepp, N. P.; Wirz, J., *J. Am. Chem. Soc.* **1988**, *110*, 7875-7876.
4. Haspra, P.; Sutter, A.; Wirz, J., *Angew. Chem. Int. Ed.* **1978**, *18*, 617-619.
5. Keefe, J. R.; Kresge, A. J., Kinetics and mechanism of enolization and ketonization. In The chemistry of enols, Rappoport, Z., Ed. Wiley: Chichester, 1990; pp 399-480.
6. Kresge, A. J., *Chem. Soc. Rev.* **1996**, 275-280.
7. Wirz, J., *Pure Appl. Chem.* **1998**, *70*, 2221–2232.
8. Chiang, Y.; Kresge, A. J.; Paine, S. W.; Popik, V. V., *J. Phys. Org. Chem.* **1996**, *9*, 361–370.
9. Wirz, J., *Chem. Unserer Zeit* **1998**, *32*, 311-322.
10. Kresge, A. J., *Acc. Chem. Res.* **1990**, *23*, 43-48.
11. Norrish, R. G. W.; Porter, G., *Nature* **1949**, *164*, 658.
12. Porter, G., Flash photolysis. In Techniques of Organic Chemistry, Part 2, Friess, S. L.; Lewis, E. S.; Weissberger, A., Eds. Interscience: New York, 1963; Vol. VII, pp 1055-1106.
13. Bonneau, R.; Wirz, J.; Zuberbühler, A. D., *Pure Appl. Chem.* **1997**, *69*, 979-992.
14. Scaiano, J. C., Nanosecond laser flash photolysis: a tool for physical organic chemistry. In Reactive Intermediate Chemistry, Moss, R. A.; Platz, M. S.; Jones, M., Jr., Eds. John Wiley & Sons: Hoboken, New Jersey, 2004; pp 847-871.
15. Klán, P.; Wirz, J., Photochemistry of Organic Compounds: From Concepts to Practice. Wiley: Chichester, 2009; p 563.
16. Bates, R. G., Determination of pH. Theory and Practise. Wiley: New York, 1973.
17. Emsley, J.; Freeman, N. J., *J. Mol. Struct.* **1987**, *161*, 193-204.
18. Meyer, K. H., *Chem. Ber.* **1912**, *45*, 2843-2864.
19. Bagno, A.; Lucchini, V.; Scorrano, G., *J. Phys. Chem.* **1991**, *95*, 345-352.
20. Chiang, Y.; Kresge, A. J.; Santaballa, J. A.; Wirz, J., *J. Am. Chem. Soc.* **1988**, *110*, 5506-5510.

21. Chiang, Y.; Kresge, A. J.; Wirz, J., *J. Am. Chem. Soc.* **1984**, *106*, 6392-6395.
22. Keefe, J. R.; Kresge, A. J.; Toullec, J., *Can. J. Chem.* **1986**, *64*, 1224-1227.
23. Chiang, Y.; Kresge, A. J.; Capponi, M.; Wirz, J., *Helv. Chim. Acta* **1986**, *69*, 1331-1332.
24. Loudon, G. M., *J. Chem. Educ.* **1991**, *68*, 973-984.
25. Toullec, J., *Adv. Phys. Org. Chem.* **1982**, *18*, 1-77.
26. Keefe, J. R.; Kresge, A. J., In Techniques of Chemistry, Investigations of Rates and Mechanisms of Reactions, Bernasconi, C. F., Ed. Wiley: New York, 1986; Vol. 6, part 1, Chapter XI.
27. Hegarty, A. F.; Dowling, J.; Eustace, S. J.; McGarraghy, H., *J. Am. Chem. Soc.* **1998**, *120*, 2290-2296.
28. Il'ichev, Y. V.; Schwörer, M. A.; Wirz, J., *J. Am. Chem. Soc.* **2004**, *126*, 4581-4595.
29. Hénin, F.; Létinois, S.; Muzart, J.; Wirz, J., *Photochem. Photobiol. Sci.* **2006**, *5*, 426-431, and references therein.
30. Haag, R.; Wirz, J.; Wagner, P. J., *Helv. Chim. Acta* **1977**, *60*, 2595-2607.
31. Schwörer, M.; Wirz, J., *Helv. Chim. Acta* **2001**, *84*, 1441-1458.
32. Goeschen, C.; Herges, R.; Richter, J.; Tokarczyk, B.; Wirz, J., *Helv. Chim. Acta* **2009**, in press, doi: 10.1002/hlca.200900191.
33. Freiermuth, B.; Hellrung, B.; Peterli, S.; Schultz, M.-F.; Wintgens, D.; Wirz, J., *Helv. Chim. Acta* **2001**, *84*, 3796-3809.
34. Chiang, Y.; Kresge, A. J.; Krogh, E. T., *J. Am. Chem. Soc.* **1988**, *110*, 2600-2607.
35. Guthrie, J. P., *Can. J. Chem.* **1993**, *71*.
36. Almstead, J. I. K.; Urwyler, B.; Wirz, J., *J. Am. Chem. Soc.* **1994**, *116*, 954-960.
37. Urwyler, B.; Wirz, J., *Angew. Chem., Int. Ed. Engl.* **1990**, *29*, 790-792.
38. Almstead, J. I. K.; Wirz, J., unpublished.
39. Chiang, Y.; Kresge, A. J.; Hochstrasser, R.; Wirz, J., *J. Am. Chem. Soc.* **1989**, *111*, 2355-2357.
40. Chiang, Y.; Kresge, A. J.; Popik, V. V., *J. Am. Chem. Soc.* **1995**, *117*, 9165-9171.
41. Chiang, Y.; Kresge, A. J.; Walsh, P. A.; Yin, Y., *J. Chem. Soc., Chem. Commun.* **1989**, 869-871.
42. Chiang, Y.; Grant, A. S.; Kresge, A. J.; Pruszynski, P.; Schepp, N. P.; Wirz, J., *Angew. Chem., Int. Ed. Engl.* **1991**, *30*, 1356-1358.
43. Chiang, Y.; Grant, A. S.; Guo, H. X.; Kresge, A. J.; Paine, S. W., *J. Org. Chem.* **1997**, *62*, 5363-5370.
44. Andraos, J.; Chiang, Y.; Grant, A. S.; Guo, H.-X.; Kresge, A. J., *J. Am. Chem. Soc.* **1994**, *116*, 7411-7412.
45. Chiang, Y.; Grant, A. S.; Guo, H.-X.; Kresge, A. J.; Paine, S. W., *J. Org. Chem.* **1997**, *62*, 5363-5370.
46. Capponi, M.; Gut, I. G.; Hellrung, B.; Persy, G.; Wirz, J., *Can. J. Chem.* **1999**, *77*, 605-613.
47. More O'Ferrall, R.; Quirke, A. P., *Tetrahedron Lett.* **1989**, *30*, 4885-4888.
48. Chiang, Y.; Kresge, A. J.; Tang, Y. S.; Wirz, J., *J. Am. Chem. Soc.* **1984**, *106*, 460-462.
49. Chiang, Y.; Kresge, A. J.; Schepp, N. P., *J. Am. Chem. Soc.* **1989**, *111*, 3977-3980.
50. Keeffe, J. R.; Kresge, A. J.; Schepp, N. P., *J. Am. Chem. Soc.* **1990**, *112*, 4862-4868.

51. Keeffe, J. R.; Kresge, A. J.; Schepp, N. P., *J. Am. Chem. Soc.* **1988**, *110*, 1993-1995.
52. Pruszynski, P.; Chiang, Y.; Kresge, A. J.; Schepp, N. P.; Walsh, P. A., *J. Phys. Chem.* **1986**, *90*, 3760-3766.
53. Chiang, Y.; Kresge, A. J.; Meng, Q.; More O'Ferrall, R. A.; Zhu, Y., *J. Am. Chem. Soc.* **2001**, *123*, 11562-11569.
54. Jefferson, E. A.; Keefe, J. R.; Kresge, A. J., *J. Chem. Soc., Perkin Trans. 2* **1995**, 2041-2046.
55. Keefe, J. R.; Kresge, A. J.; Yin, Y., *J. Am. Chem. Soc.* **1988**, *110*, 8201-8206.
56. Chiang, Y.; Guo, H.-X.; Kresge, A. J.; Tee, O. S., *J. Am. Chem. Soc.* **1996**, *118*, 3386-3391.
57. Chiang, Y.; Kresge, A. J.; Meng, Q.; Morita, Y.; Yamamoto, Y., *J. Am. Chem. Soc.* **1999**, *121*, 8345-8351.
58. Chang, J. A.; Kresge, A. J.; Nikolaev, V. A.; Popik, V. V., *J. Am. Chem. Soc.* **2003**, *2003*, 6478-6484.
59. Chiang, Y.; Kresge, A. J.; Nikolaev, V. A.; Popik, V. V., *J. Am. Chem. Soc.* **1997**, *119*, 11183-11190.
60. Chiang, Y.; Kresge, A. J.; Nikolaev, V. A.; Onyido, I.; Zeng, X., *Can. J. Chem.* **2005**, *83*, 68-76.
61. Chang, J. A.; Chiang, Y.; Keefe, J. R.; Kresge, A. J.; Nikolaev, V. A.; Popik, V. V., *J. Org. Chem.* **2006**, *71*, 4460-4467.
62. Gut, I. G.; Scheibler, L. C.; Wirz, J., unpublished work.
63. McCann, G. M.; McDonnell, C. M.; Magris, L.; More O'Ferrall, R. A., *J. Chem. Soc., Perkin Trans. 2* **2002**, 784-795.
64. Chiang, Y.; Hojatti, M.; Keeffe, J. R.; Kresge, A. J.; Schepp, N. P.; Wirz, J., *J. Am. Chem. Soc.* **1987**, *109*, 4000-4009.
65. Chiang, Y.; Kresge, A. J.; Walsh, P. A., *J. Am. Chem. Soc.* **1986**, *108*, 6314-6340.
66. Andraos, J.; Chiang, Y.; Kresge, A. J.; Popik, V. V., *J. Am. Chem. Soc.* **1997**, *119*, 8417-8424.
67. Andraos, J.; Chiang, Y.; Kresge, A. J.; Pojarlieff, I. G.; Schepp, N. P.; Wirz, J., *J. Am. Chem. Soc.* **1994**, *116*, 73-81.
68. Chiang, Y.; Kresge, A. J.; Popik, V. V.; Schepp, N. P., *J. Am. Chem. Soc.* **1997**, *119*, 10203-10212.
69. Chiang, Y.; Kresge, A. J.; Pruszynski, P.; Schepp, N. P.; Wirz, J., *Angew. Chem., Int. Ed. Engl.* **1990**, *102*, 810-812.
70. Chiang, Y.; Kresge, A. J.; Schepp, N. P.; Xie, R.-Q., *J. Org. Chem.* **2000**, *65*, 1175-1180.
71. Chiang, Y.; Guo, H.-X.; Kresge, A. J.; Richard, J. P.; Toth, K., *J. Am. Chem. Soc.* **2003**, *125*, 187-194.
72. Capponi, M. Bestimmung von Keto-Enol Gleichgewichten mittels Blitzlichtphotolyse: Phoron und Phenol. PhD thesis, University of Basel, 1986.
73. Gut, I. G.; Wirz, J., *Angew. Chem., Int. Ed. Engl.* **1994**, *33*, 1153-1156.
74. Brønsted, J. N.; Pedersen, K., *Z. Phys. Chem.* **1924**, *108*, 185-235.
75. Brønsted, J. N., *Chem. Rev.* **1928**, *5*, 231-338.
76. Bishop, D. M.; Laidler, K. J., *J. Chem. Phys.* **1965**, *42*, 1688-1691.
77. Kresge, A. J., *Chem. Soc. Rev.* **1973**, *2*, 475-503.
78. Bell, R. P., The Proton in Chemistry. Chapman and Hall: London, 1973.
79. Hellrung, B.; Hörmann, A.; Schultz, M.-F.; Wintgens, D.; Wirz, J., *unpublished work.*
80. Keeports, D., *J. Chem. Educ.* **2005**, *82*, 999.
81. Keeports, D., *J. Chem. Ed.* **2006**, *83*, 1290.
82. Eigen, M., *Angew. Chem.* **1963**, *75*, 489-508.

83. Marcus, R. A., *J. Phys. Chem.* **1968**, *72*, 891-899.
84. Cohen, A. O.; Marcus, R. A., *J. Phys. Chem.* **1968**, *72*, 4249-4256.
85. Benson, S. W.; Cruickshank, F. R.; Golden, D. M.; Haugen, G. R.; O'Neal, H. E.; Rodgers, A. S.; Shaw, R.; Walsh, R., *Chem. Rev.* **1968**, *68*, 279-324.
86. Guthrie, J. P., *J. Phys. Chem. A* **2001**, *105*, 9196-9202.